NASA Technical Memorandum 78717

PREDICTION OF AIRCRAFT SIDELINE NOISE ATTENUATION

by

William E. Zorumski

June 1978

National Aeronautics and Space Administration

Langley Research Center
Hampton, Virginia 23665

PREDICTION OF AIRCRAFT SIDELINE NOISE ATTENUATION

by

WILLIAM E. ZORUMSKI
NASA-Langley Research Center

SUMMARY

A computational study is made using the recommended ground effect theory by Pao, Wenzel, and Oncley. It is shown that this theory adequately predicts the measured ground attenuation data by Parkin and Scholes, which is the only available large data set. It is also shown, however, that the ground effect theory does not predict the measured lateral attenuations from actual aircraft flyovers. There remain one or more important lateral effects on aircraft noise, such as sideline shielding of sources, which must be incorporated in the prediction methods. Experiments at low elevation angles (0^{o} to 10^{o}) and low-to-intermediate frequencies are recommended to further validate the ground effect theory.

LIST OF SYMBOLS

a incoherence factor

c_a ambient speed of sound, m/s

$C(\omega)$ coherence function

f frequency, Hz

H source altitude, m

h receiver altitude, m

k wave number, $2\ f/c_a$

R magnitude of the complex reflection coefficient

r direct path length between source and base of receiver, m

r_1 direct path length between source and receiver, m

r_2 reflected path length equivalent to direct path between image source and receiver, m

α phase of complex reflection coefficient

Γ plane wave reflection coefficient

γ elevation angle from base of receiver to source, deg.

ξ distance parameter

η frequency parameter

θ angle of incidence, deg.

$\nu = \nu_1 + \nu_2$, specific complex ground admittance function

ρ_o density of air at ground level, kg/m^3

σ ground flow resistance, $Ns/m^4 = (kg/m^3)/s$

$\omega = 2\pi f$, circular frequency, radian/s

GROUND EFFECT PREDICTION

Geometry

The prediction of ground effects is based on the geometry of figure 1. A Source S located at an altitude H over a ground plane emits sound which is propagated to a receiver R. The sound travels along the direct part r_1 and a reflected path. The reflected path is equivalent to the same sound traveling from the image source I along a path r_2. Here, only long ranges are considered so that $(h/r) << 1$. Under these conditions, $\sin \gamma \simeq \cos \theta$, $r_1 \simeq r_2 \simeq r$, and the path difference $r_2 - r_1 \simeq 2h\sin \gamma = 2hH/r$

Prediction Formula

The basic prediction formula given by Pao, Wenzel, and Oncley (ref. 1) is

$$\bar{p}_{gr}^2 = \bar{p}_{ff}^2(1 + 2RC(\omega) \cos[\alpha + k(r_2 - r_1) + R^2) \qquad (1)$$

where p_{ff}^2 is the mean-squared pressure in the free-field, p_{gr}^2 is the mean-squared pressure with the ground effect, $Re^{i\alpha}$ is the complex reflection coefficient, k is the wave number, and $C(\omega) = \exp\{-[ak(r_2-r_1)]^2\}$ is a dimensionless measure of the coherence between the direct and reflected sounds. The reflection coefficient may depend on frequency, incidence angle, and distance. The constant, or incoherence factor a, is set to 0.01 so that the coherence $C(\omega)$ is 37% when $r_2 - r_1 = 16$ wavelengths.

Ground Admittance

The basic property of the ground surface is the ground admittance. The normalized admittance is calculated from the eimpirical formula of Delaney and Bazley (ref. 2), which is

$$\nu = \left\{ 1 + [6.86\eta]^{-0.75} + i\,[4.36\,\eta]^{-0.75} \right\}^{-1}, \tag{2}$$

where

$$\eta = 2\pi\rho_0\, f/\sigma \tag{3}$$

ρ_0 is the ground level air density, f is the frequency, and σ is the ground flow resistance. Figure 2 shows $\nu = \nu_1 + i\nu_2$ as a function of η.

Plane-Wave Reflection

The plane-wave reflection coefficient is

$$\Gamma = (\sin\gamma - \nu)/(\sin\gamma + \nu) \tag{4}$$

A plane-wave ground effect theory results from using $\Gamma = Re^{i\alpha}$ in equation 1. This theory erroneously predicts $p_{gr}^2 = 0$ when $\sin\gamma = 0$.

Ingard-Rudnick Theory

The Ingard-Rudnick theory adds a term to the plane-wave reflection coefficient. Their equation is

$$Re^{i\alpha} = \Gamma + \frac{2i}{kr}\,\frac{(1+\nu\sin\gamma)}{(\sin\gamma+\nu)^3} \tag{5}$$

This equation removes the erroneous zero pressure for ground-to-ground propagation, but adds a dependence of the ground effect on distance as well as frequency and incidence angle. The distance effect can be incorporated through the parameter $\xi = \frac{\sigma r}{\rho_0 c_0}$ which does not depend on frequency. Since $kr = \xi\eta$, equations (2) and (3) depend on two independent parameters, ξ and η. For large values of kr, the Ingard-Rudnick theory

approaches the plane-wave theory.

Chien-Soroka Theory

The Chien-Soroka theory has

$$Re^{i\alpha} = \Gamma + (1 - \Gamma)\ F(\tau) \tag{6}$$

where

$$\tau = \sqrt{\frac{kr}{2i}}\ (\sin\gamma + \nu), \tag{7}$$

$$F(\tau) = 1 - \sqrt{\pi}\ \tau\ W(i\tau), \tag{8}$$

and W is the complex error function

$$W(z) = \frac{i}{\pi} \int_{-\infty}^{\infty} \frac{e^{-t^2}}{z-t}\ dt,\ \mathrm{Im}(z)>0 \tag{9}$$

The Chien-Soroka theory reduces first to the Ingard-Rudnick theory and then to the plane-wave theory as $|\tau|$ becomes large. When τ has a positive real part, the asymptotic expansion for $F(\tau)$ is

$$F(\tau) \sim \frac{1}{2\tau^2} - \frac{3}{(2\tau^2)^2} + \cdots \tag{10}$$

Limits of Theories

Parameters.- Assuming $\sigma = 2.5 \times 10^5$ N s/m^4 and $\rho_0 = 1.225$ kg/m^3, the parameter η has a range of $1\text{-}32 \times 10^{-3}$ for frequencies of 31.5 - 1000 Hz where ground attenuation effects are important. The parameter $\xi = (\sigma r/\rho_0 c_a)$ is about 10^6 at 1 nautical mile. Thus, at 1/4 n mi., the parameter $kr = \xi\eta$ has a range .25 - 8×10^3.

One-Percent Errors.- The plane-wave theory involves neglecting the first term in equation (10). If this approximation has an error of E%, then $|\tau|^2 \geq 50/E$. Similarly, if the first term is included to give the Ingard-Rudnick theory, but the second term is neglected, an error of E% requires that $|\tau|^2 \geq (75/E)^{1/2}$. From the definition of τ, a limit on $\sin\gamma$ may be

found as a function of η and ξ. This limit is

$$\sin\gamma \geq [2|\tau|^2/(\xi\eta) - \nu_2^2]^{1/2} - \nu_1 \qquad (11)$$

If the term on the right of equation (11) is negative or imaginary, all angles are permitted.

Figure 3 shows limits defined by equation (11) for 1 percent error at $\xi = 0.25 \times 10^6$. A limiting curve where the Ingard-Rudnick theory is within 1 percent of the plane-wave theory is shown by a dashed line. The solid curve near the abscissa shows the region where a ground wave (see ref. 1) exists so that the Chien-Soroka theory must be used.

Band Averaging

Equation (1) is valid for spectrum levels; however, bands are almost always used in practice so that equation (1) must be integrated over the band. Numerical integration requires a great deal of computation; however, if the assumption is made that R and α vary slowly within the band, an average can be explicitly given for the term $\cos[\alpha+2kh \sin\gamma]$. This average is

$$\overline{\cos[\alpha+2kh \sin\gamma]} = \cos[\alpha+2kh \sin\gamma] \frac{\sin[.231kh \sin\gamma]}{[.231kh \sin\gamma]} \qquad (12)$$

for a 1/3 octave band. Figure 4 shows a computation of the ground effect with the plane-wave theory for the 250 Hz band center and band limit frequencies. The band average ground effect is also shown on figure 4. This figure shows that the primary effect of the bandwidth is to fill in dips in the ground effect curve which are caused by cancellation. The spectral curves on figure 4 also have a finite amount of cancellation due to partial incoherence of the direct and reflected wave.

Figure 5 shows the ground effect for typical 1/3 octave bands where large attenuations are found. The results shown in figure 5 are for a 1.2

meter microphone height with $\rho_o = 1.225$ kg/m^3 and $\sigma = 2.5 \times 10^5$ N s/m^4. The primary difference between these curves is the number of dips, or points of large cancellation. The limits of the plane-wave theory, as compared to the complete theory at a distance of 1/4 nautical mile, are also shown in figure 5 by the differences between the curves for each prediction method.

APPLICATION TO AIRCRAFT SIDELINE NOISE PREDICTION

Ground-to-Ground Propagation

Chessell[3] has shown that the ground resistance σ must be about 3×10^5 N s/m^4 for the Delaney-Bazley formula to give a best fit to measured ground impedance data. Here, a value of σ will be chosen such that the Chien-Soroka theory gives a best fit to the Parkin and Scholes[4,5] ground-to-ground propagation data. Parkin and Scholes have conducted major experiments at two sites: Radlett and Hatfield. Figure 6 shows the schematic microphone array used by Parkin and Scholes. The source is a small jet engine with the engine axis 1.83 m above the ground surface. All microphones are 1.52 m above the ground and are placed at distances as shown in the figure. The distance between adjacent microphones is such that a 5 dB change in the noise level will occur due to spherical spreading. This change is extracted from the measured data which will be presented here, as are the effects of atmospheric absorption of sound. Figure 7 shows how the first microphone in the Parkin and Scholes experiment is used as a reference. In the experiment all data are referred to the first microphone. Thus, in making a theoretical comparison, a spectrum is predicted for the first microphone and the microphone of interest. These predictions relate the spectrum with ground effect to the free-field spectrum. The reference microphone spectrum is then subtracted out.

Since the prediction for the reference microphone shows a pronounced dip at 400 Hz, the resulting comparison curve has a peak at this point. It will be seen later that this peak does not appear in the data; however, its absence could be due to the ground condition in the immediate neighborhood of the reference microphone.

Figure 8 shows the predictions, using the Chien-Soroka theory, compared to the Radlett data. The prediction is poor at short distances. The errors are due to the predicted dips for the reference microphone. At longer distances, it can be seen that the prediction accounts for the major characteristics of the data. The long range data show evidence of the 400 Hz peak due to subtracting out the reference micrphone. Also, there is a variation in the data between summer and winter. This variation could possibly be attributed to a change in the ground resistance, however, no attempt was made to provide a precise fit of the theory to the data by varying this parameter. It is significant that the long range data are predicted fairly well by the theory. It is in this range of distances, 500 to 1000 m, that aircraft sideline noise is important. Figure 9 shows a comparison of the predictions to the Parkin and Scholes data at Hatfield. Again, using a ground resistance parameter of 2.5×10^5 N s/m^4 gives a fair comparison to the data at long ranges.

Air-to-Ground Propagation

The case of primary interest for aircraft noise is air-to-ground propagation. In order to have a convenient practical reference, the estimated jet mixing noise spectrum will be used in studying the ground effect for this situation. Figure 10 shows this Concorde noise spectrum with a D-weighting function added and 7 dB added. These modifications make the overall level of the figure 10 spectrum curve roughly equal to the perceived noise in PNdB minus

the overall sound pressure level. Figure 11 shows the predicted ground effect on the weighted spectrum of figure 10. At low evaluation angles γ there is a pronounced attenuation of the frequencies in the 200-1000 Hz region, however, at the high frequencies, the ground does not reduce the free-field levels. At higher elevation angles, the predicted ground effect quickly dies away, although alternate bumps and dips in the spectrum remain due to cancellation and reinforcement effects.

The curves of figure 11 may be integrated to find the variation in perceived noise with elevation angle. When this is done, the absence of a high frequency ground attenuation places a limit on the amount of perceived noise attenuation which is observed.

Concorde Lateral Attenuation

Integrals of curves such as in figure 11 have been made to compare the predicted ground attenuation of Concorde perceived noise to actual sideline data. These data, from reference 6, were taken at a fixed .35 n mi sideline with 1.2 m microphones with the aircraft flying past at successively higher altitudes. No absolute units are given for the Concorde data so that a least-squares fit of the prediction curve was used for comparison of the variations of the perceived noise with elevation angle. Since the data have a distance effect which is proportional to $(\cos \gamma)^{-2}$, this term was used to modify the theory to obtain the solid curve in figure 12. The broken curve shows the predicted variation of the ground effect on perceived Concorde noise with elevation angle only. It is apparent that, although the data are badly scattered, the fit between ground effect theory and measured lateral attenuation is poor. The benefit, or difference between overhead noise and sideline noise, due to ground effect rapidly decreases in the range of

angles $0<\sin\gamma<0.1$, while the observed lateral position effects on the Concorde noise is greater at these angles and does not disappear as quickly.

Since there is a rapid variation in predicted ground effect at small angles, figure 13 show the range of angles $0 \leq \sin \leq 0.1$ on an expanded scale. If the overhead position, shown on figure 13 as an asymptote, is used as a reference for the variation of ground attenuation with elevation angle, figure 13 shows that the benefit varies from about 5 dB at the very low angles ($\sin\gamma<.01$) to about 1.5 dB at low angles ($\sin\gamma<.1$).

As an alternate comparison of the ground attenuation effect to the Concorde data, the purely empirical curves by Walker in reference 7 were used to modfy the weighted Concorde spectrum in figure 10. Figure 14 shows the modified spectra for angles of 2°, 4°, 8°, 16°, and 32°. These curves show much more low frequency noise reduction than do the curves with only the predicted ground effect. This extra reduction is expected since the empirical curves of reference 7 were developed from lateral noise measurements on aircraft and naturally contain a number of effects other than the ground effect. It is important to note that the primary differences between the empirical lateral attenuation curves of figures 14 and the predicted ground attenuation curves of figure 11 are in the low and intermediate frequencies of less than 1000 Hz. Figure 15 shows the variation of the Concorde perceived noise with elevation angle when the reference 7 empirical curves are used for prediction. The Chien-Soroka ground effect prediction is also shown on figure 15 for comparison to the empirical data. The empirical lateral effect predictions show greater lateral effect benefits at the low angles which is consistent with the Concorde data.

CONCLUSIONS

The Chien-Soroka theory recommended by Pao, Wenzel, and Oncley for use in aircraft noise prediction shows fair-to-good agreement with the ground-to-ground propagation data by Parkin and Scholes. This same theory predicts that, for a supersonic transport such as the Concorde, the ground effect will reduce the .35 nautical mile sideline perceived noise by about 5 dB when the aircraft is at very low elevation angles. This benefit quickly reduces to about 1.5 dB as the aircraft rises to elevation angles above 6°.

Lateral noise measurements on the Concorde and other aircraft show a reduction in sideline noise similar to that predicted by ground effect theory; however, the magnitude of the measured latearal effect is greater at low elevation angles than is predicted by ground effect theory alone. Both the ground effect theory and the measured lateral attenuations show that the measured noise reductions occur for frequency bands below 1000 Hz. The differences between predicted and measured lateral ground effects is most pronounced at low elevation angles and low-to-intermediate frequencies.

Although the Parkin and Scholes data has been useful in validating the ground effect theory, there is no available data set to validate the theory in the very low ($\sin\gamma<.01$) to low ($\sin\gamma<.1$) elevation angle range where the theory predicts a rapid decrease in the ground attenuation effect. Also, there is no data set wherein both ground impedance and ground attenuation have both been measured at the same site. Therefore, an experiment should be conducted with both types of measurement. The low elevation angles and low-to-intermediate frequency range should be emphasized in the proposed experiment. It is anticipated that this ground effect experiment will not resolve the present discrepancy between predicted sideline ground attenuation and measured

lateral effects of flyover noise. Other phenomena such as source shielding should be considered as potential sources of lateral effects.

REFERENCES

1. Pao, S. P.; Wenzel, A. R.; and Oncley, P. B.: Prediction of Ground Effects on Aircraft Noise. NASA TP-1104, 1978.

2. Delaney, M. E.; and Bazley, E. N.: Acoustic Properties of Fibrous Absorbent Material. Applied Acoustics, 3 pp. 105-116, 1970.

3. Chessell, C. I.: Propagation of Noise Along a Finite Impedance Boundary. J. Acous. Soc. Am., 62, 4, pp. 825-834, 1977.

4. Parkin, P. H.; and Scholes, W. E.: The Horizontal Propagation of Sound from a Jet Engine Close to the Ground at Radlett. J. Sound Vib., 1, p. 1, 1974.

5. Parkin, P. H.; and Scholes, W. E.: The Horizontal Propagation of Sound from a Jet Engine Close to the Ground at Hatfield. J. Sound Vib., 2, p. 353, 1975.

6. Cooper, J. G.: Lateral Noise Propagation Acoustic Report 526. British Aircraft Corporation Commercial Aircraft Division. Weybridge, Surrey, United Kingdom, April 1977.

7. Walker, David Q.: An Analysis of Aircraft Flyover Noise. Bolt Beranek and Newman Report 3698, January 1978.

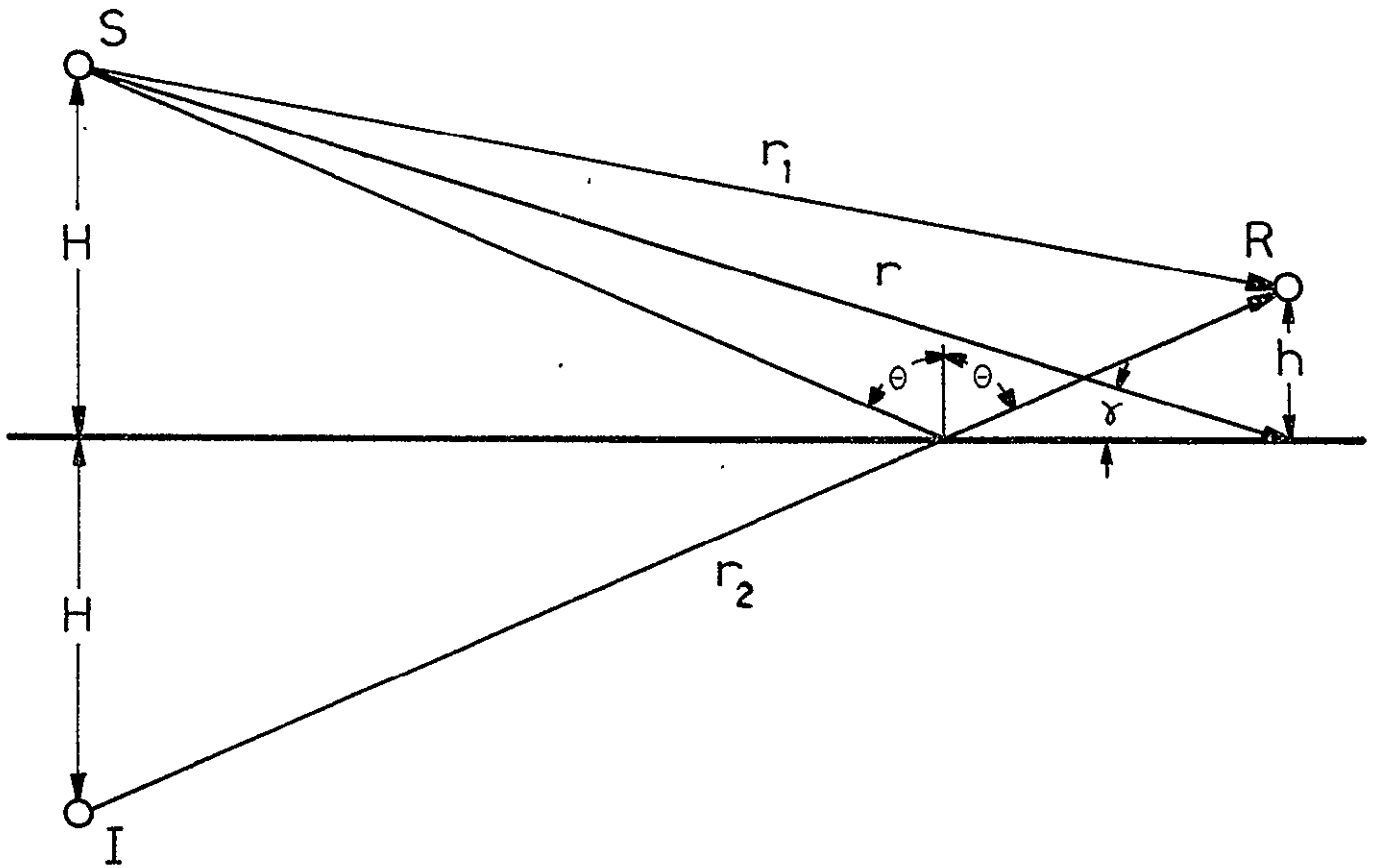

FIGURE 1. Ground effect geometry

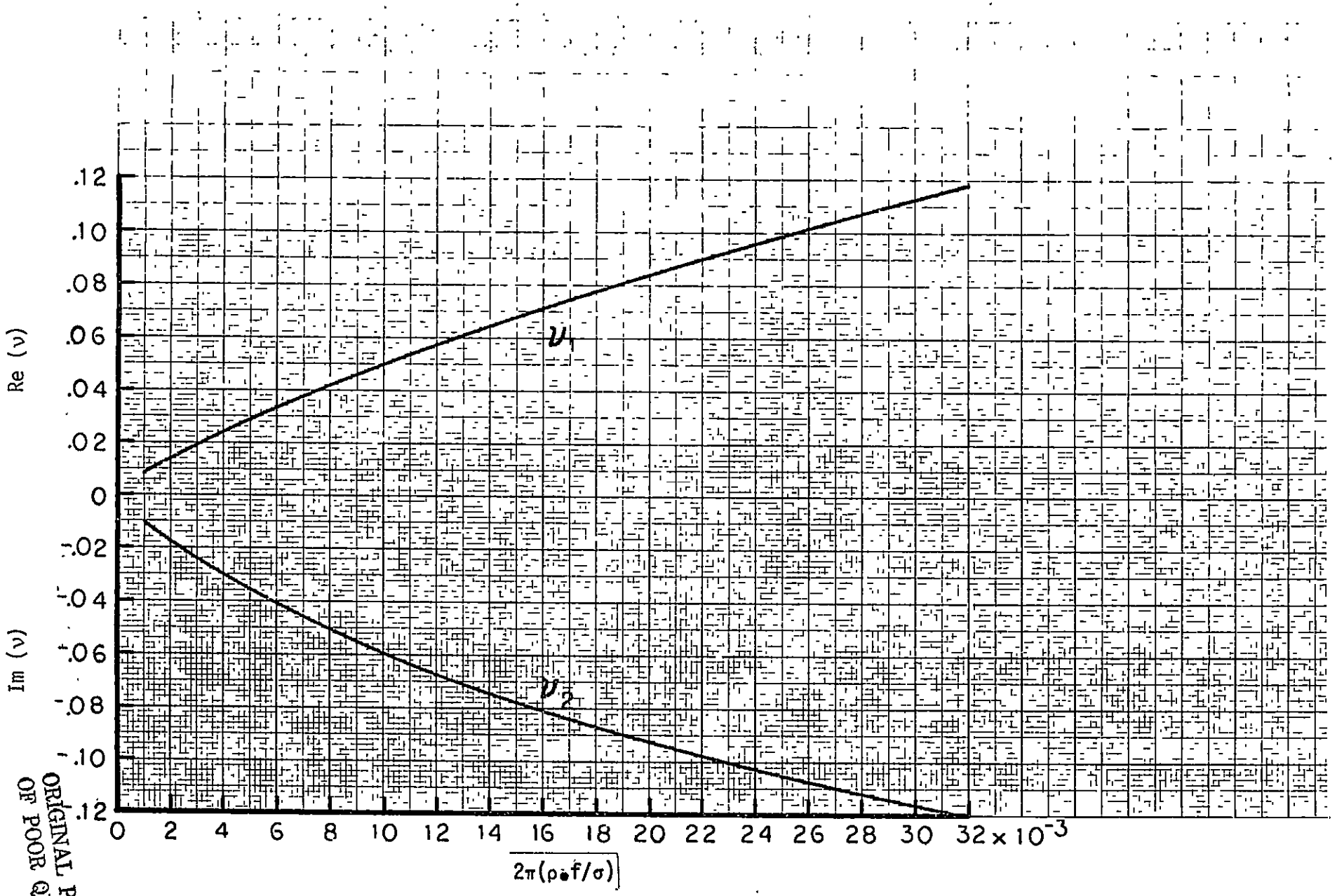

Figure 2. Ground admittance predicted by the Delaney & Bazley formula

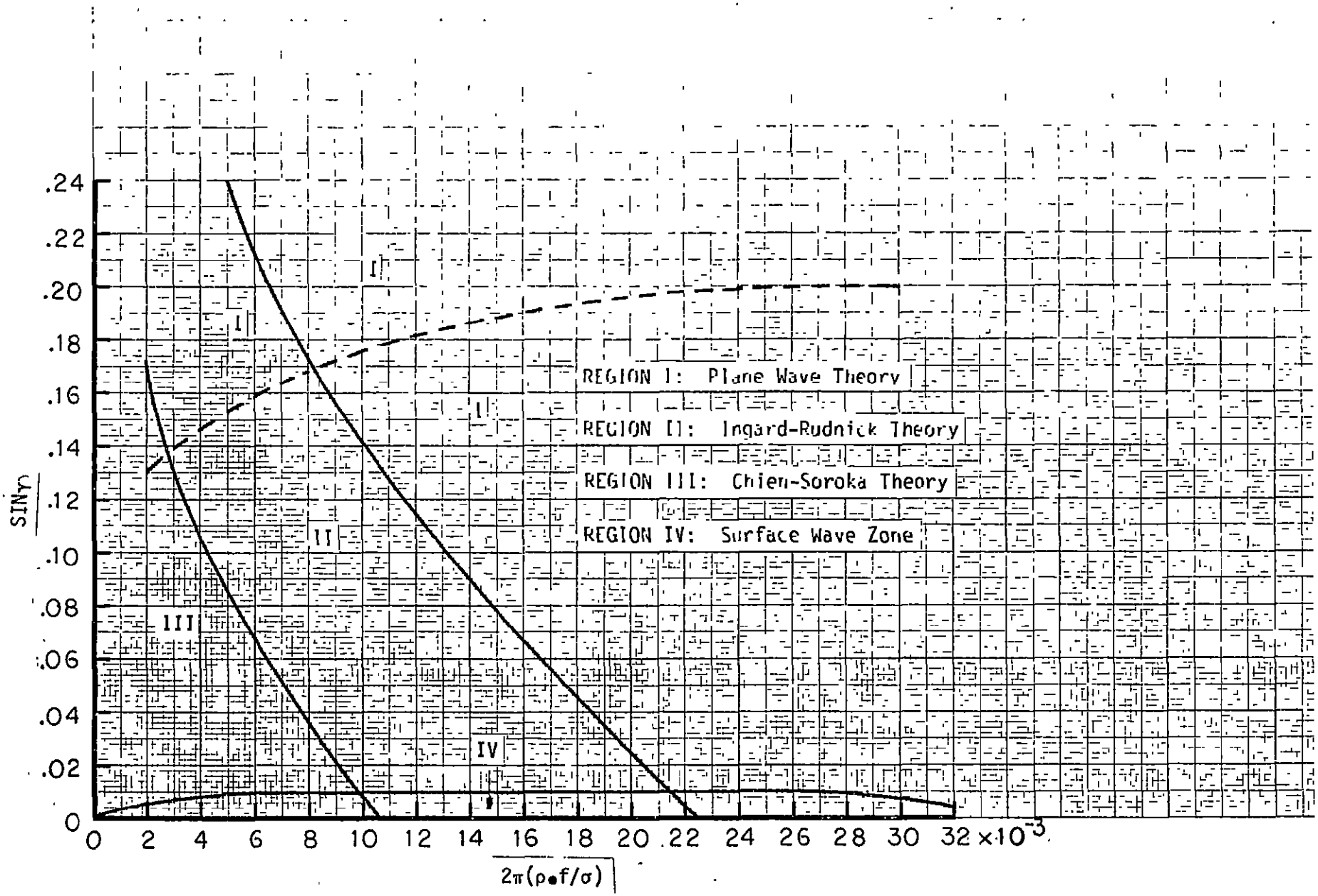

Figure 3. Limits of ground effect theories for one-percent errors.

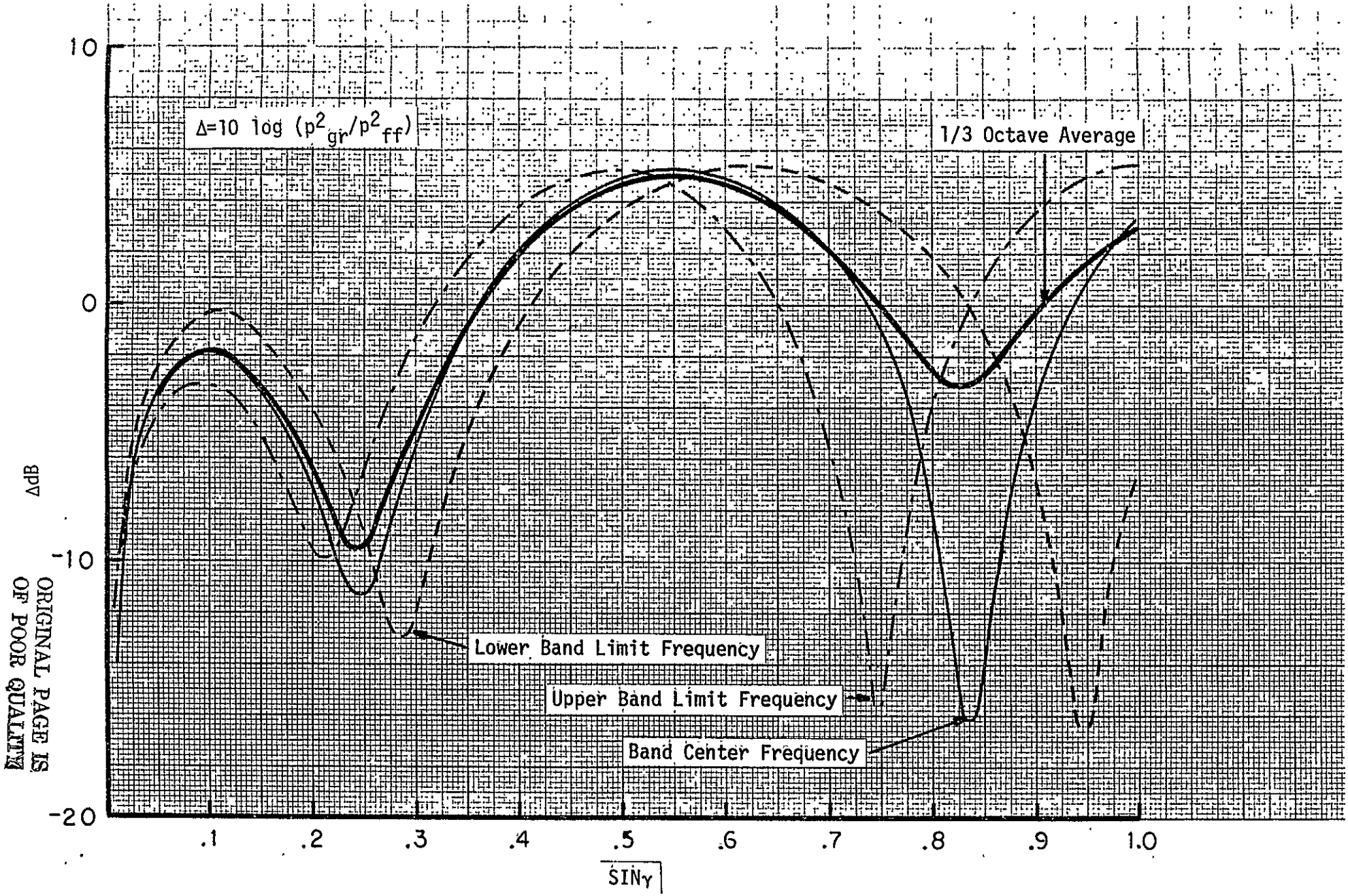

Figure 4. Ground effect on free-field spectrum levels in 1/3 octave band centered at 250 Hz. 1.2 m microphone at .25 n mi with ground resistance of 2.5×10^5 N s/m^4.

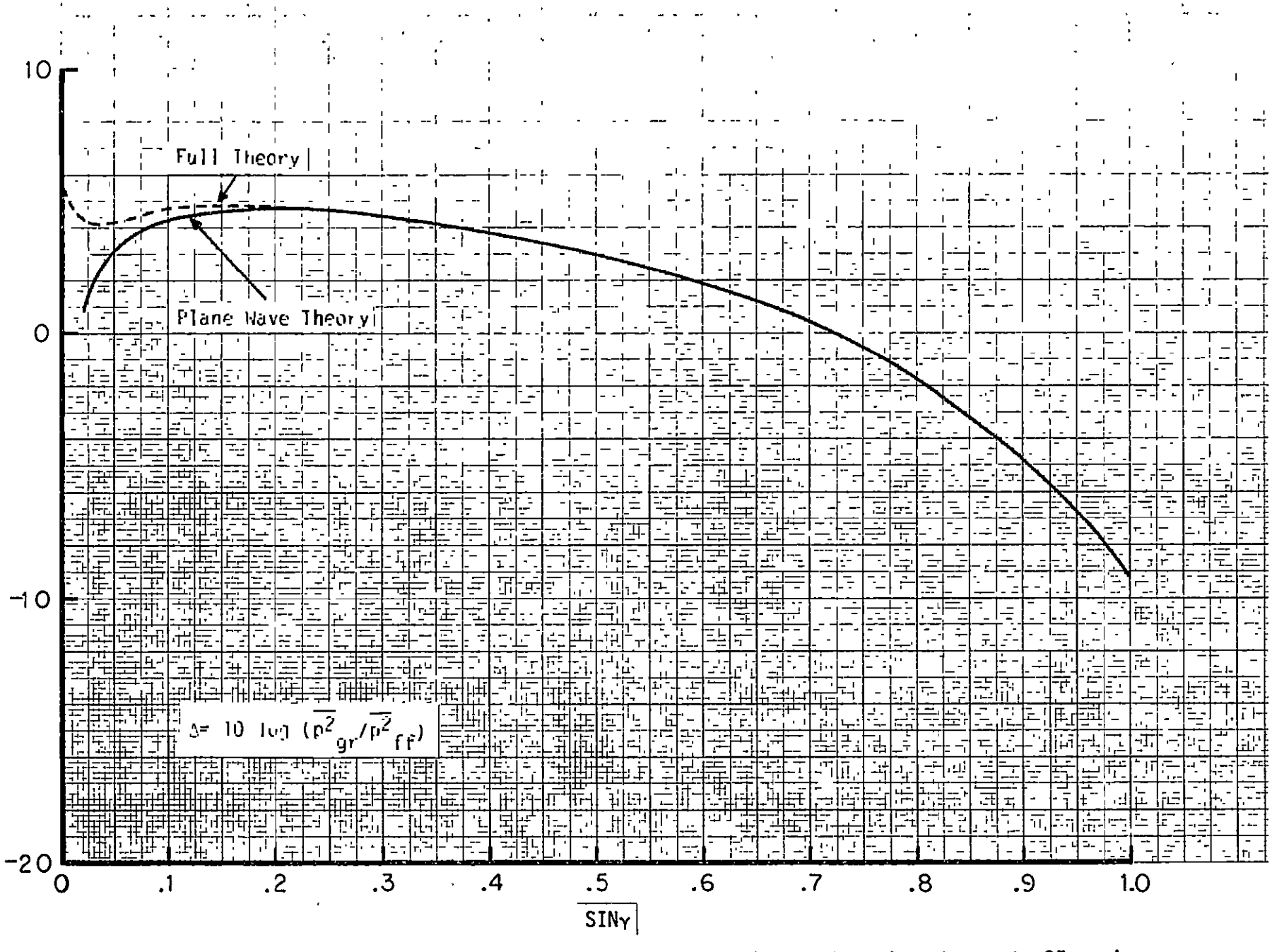

Figure 5. Ground effect on free-field 1/3 octave band levels. 1.2 m microphone at .25 n mi with ground admittance of 2.5×10^5 N s/m^4.

a) 63 Hz band center

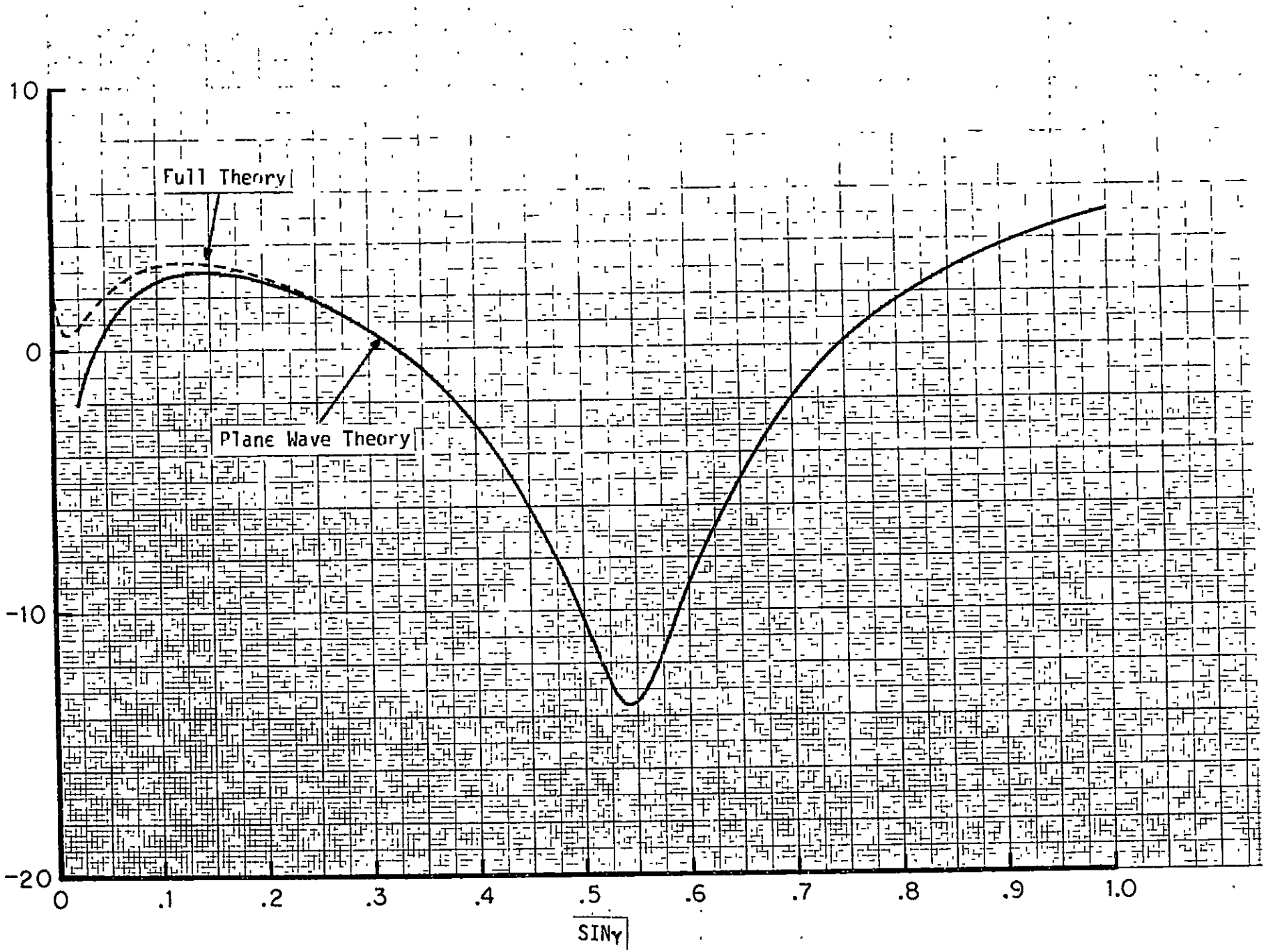

Figure 5. Ground effect on free-field 1/3 octave band levels. 1.2 m microphone at .25 n mi with ground admittance of 2.5×10^5 N s/m^4.

b) 125 Hz band center

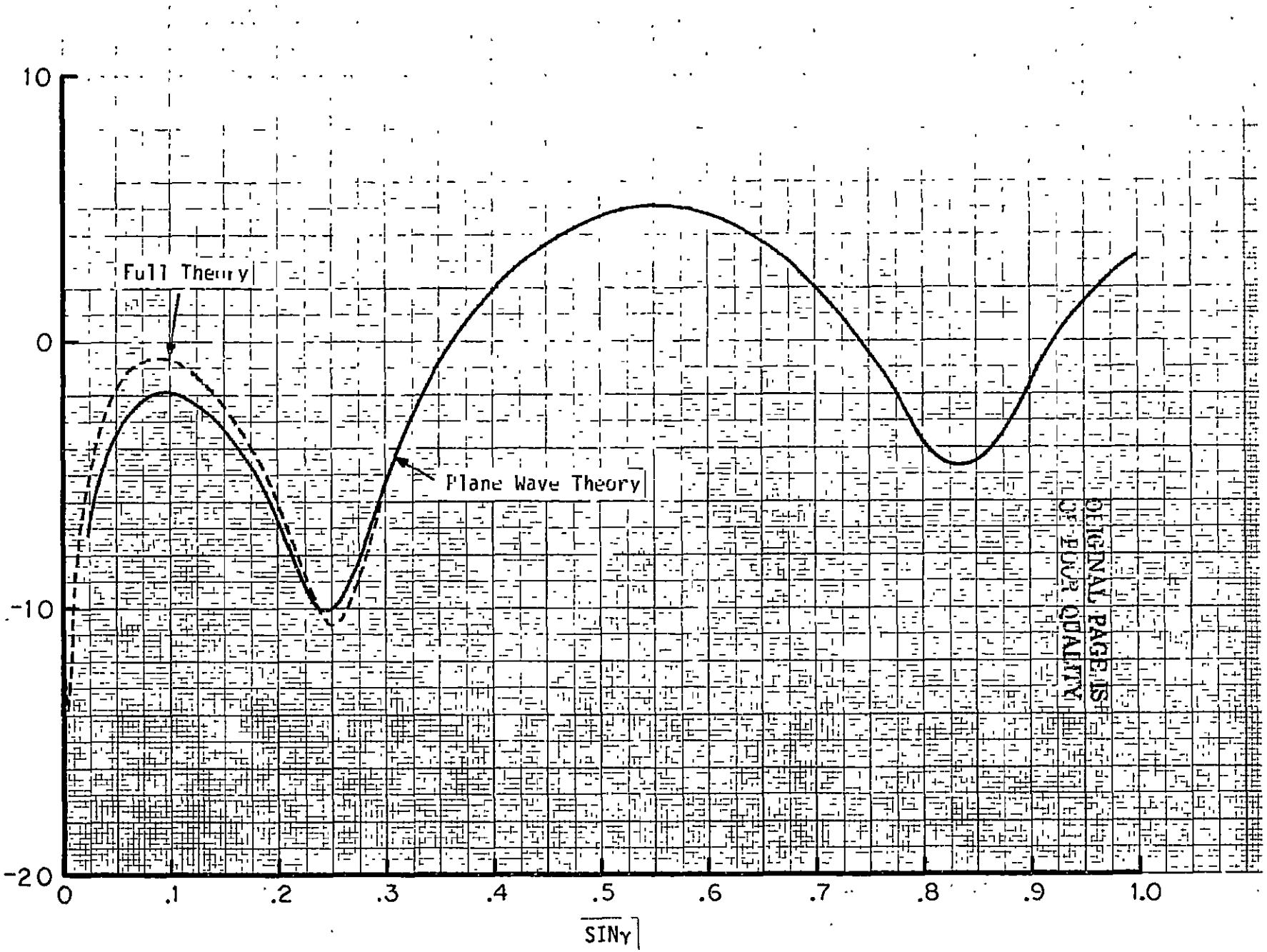

Figure 5. Ground effect on free-field 1/3 octave band levels.[4] 1.2 m microphone at .25 n mi with ground admittance of 2.5×10^5 N s/m^4.

c) 250 Hz band center

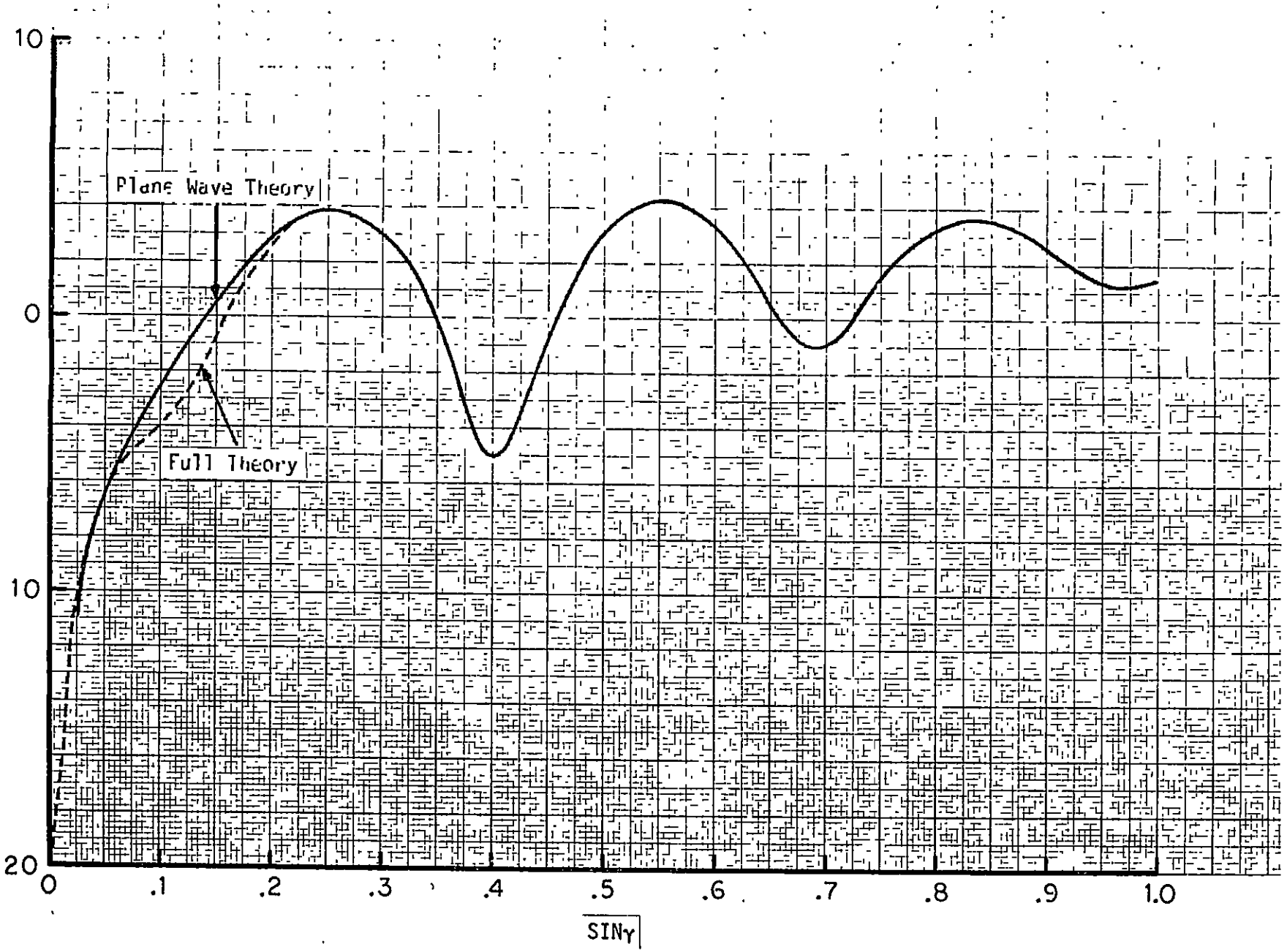

Figure 5. Ground effect on free-field 1/3 octave band levels. 1.2 m microphone at .25 n mi with ground admittance of 2.5×10^5 N s/m^4.

d) 500 Hz band center

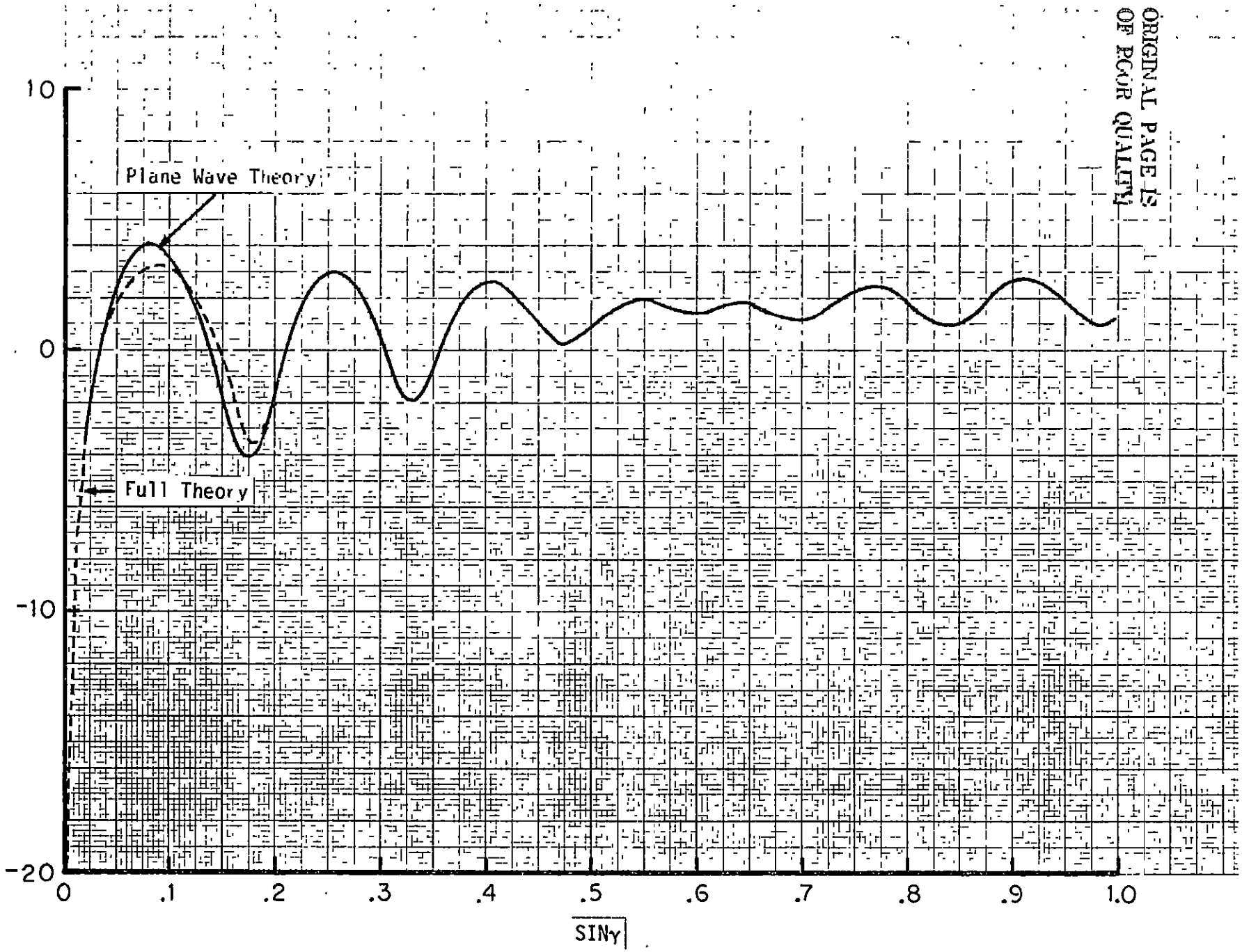

Figure 5. Ground effect on free-field 1/3 octave band levels. 1.2 m microphone at .25 n mi with ground admittance of 2.5×10^5 N s/m^4.

e) 1000 Hz band center.

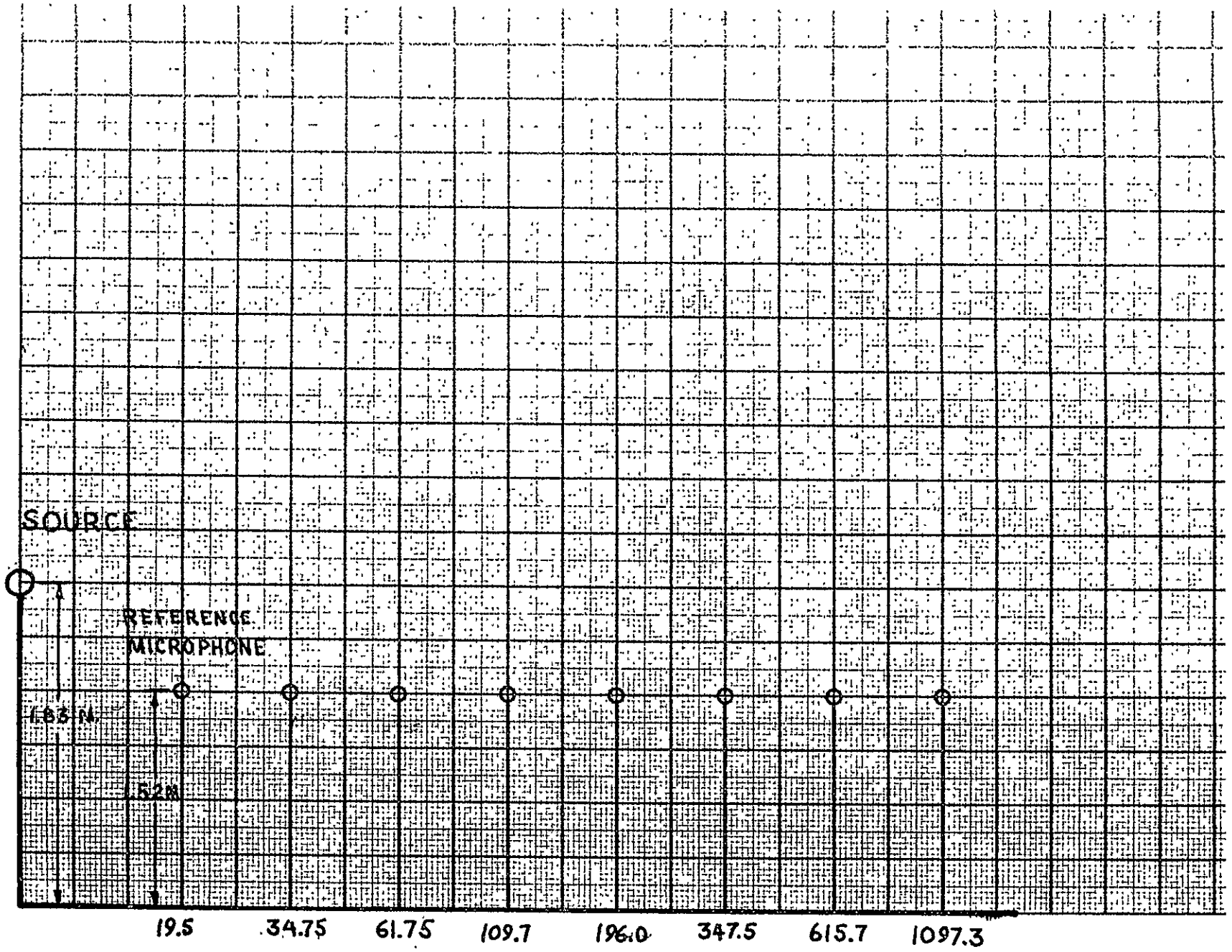

Figure 6. Microphone array used in Parkin and Scholes experiment

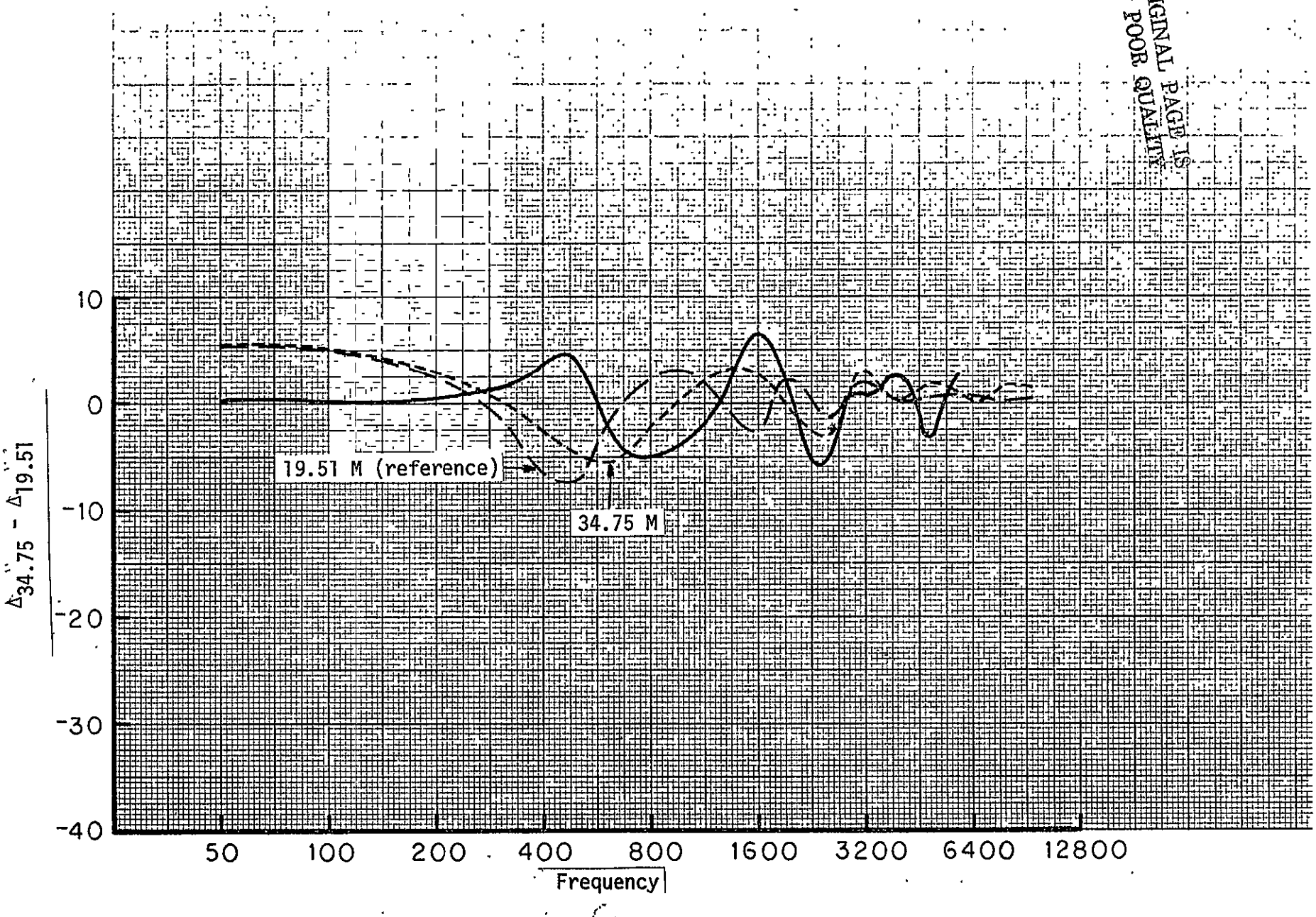

Figure 7. Method of correcting predicted 1.3 octave band levels for comparison to the Parkin and Scholes experimental data.

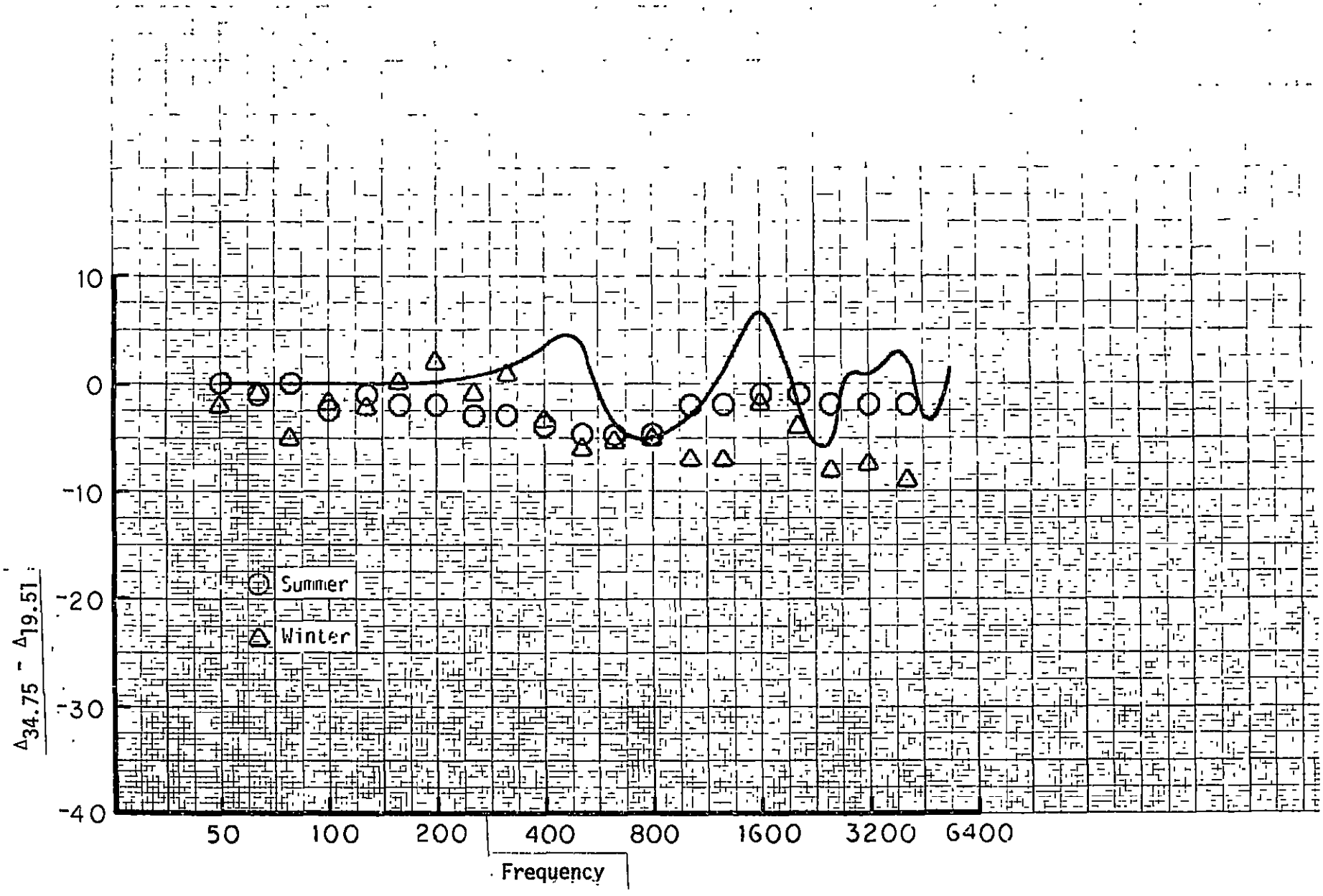

Figure 8. Comparison of Chien-Soroka theory to the Parkin and Scholes experimental data at Radlett. Ground admittance predicted by the Delaney and Bazley formula with assumed flow resistance of 2.5×10^5 N s/m^4.

a) 34.75 m microphone

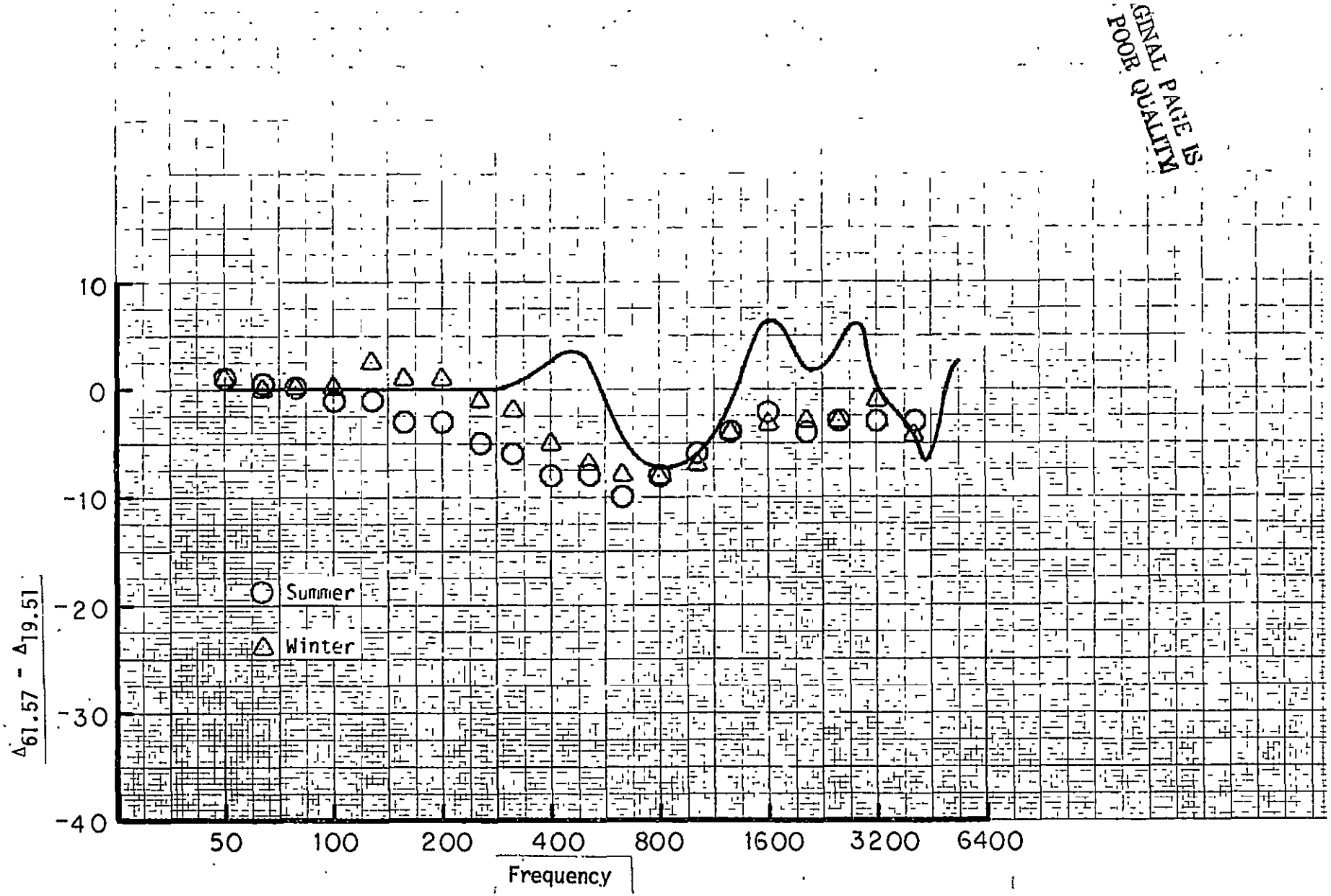

Figure 8. Comparison of Chien-Soroka theory to the Parkin and Scholes experimental data at Radlett. Ground admittance predicted by the Delaney and Bazley formula with assumed flow resistance of 2.5×10^5 N s/m^4.

b) 61.57 m microphone

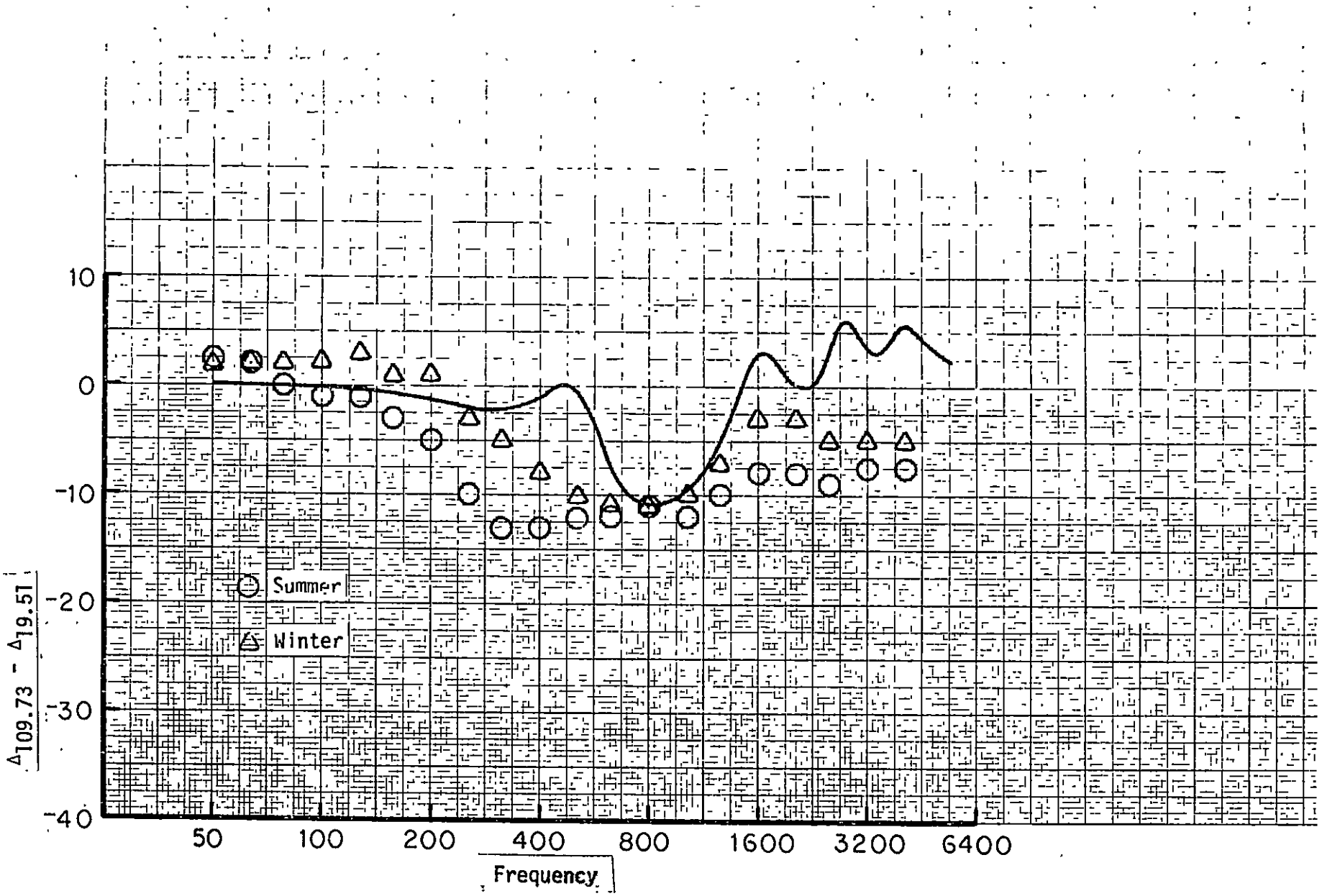

Figure 8. Comparison of Chien-Soroka theory to the Parkin and Scholes experimental data at Radlett. Ground admittance predicted by the Delaney and Bazley formula with assumed flow resistance of 2.5×10^5 N s/m^4.

c) 109.73 m microphone

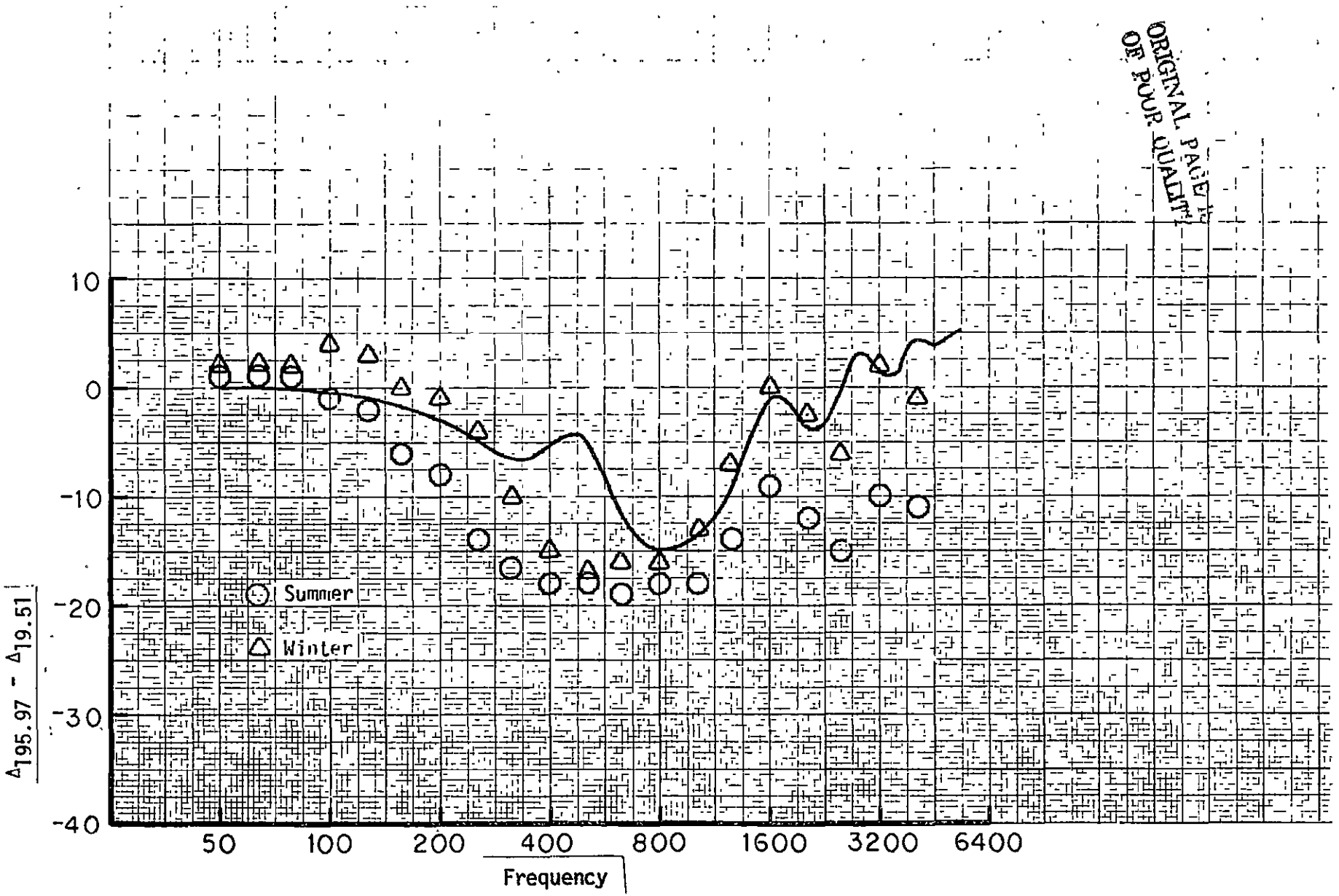

Figure 8. Comparison of Chien-Soroka theory to the Parkin and Scholes experimental data at Radlett. Ground admittance predicted by the Delaney and Bazley formula with assumed flow resistance of 2.5×10^5 N s/m^4.

d) 195.97 m microphone

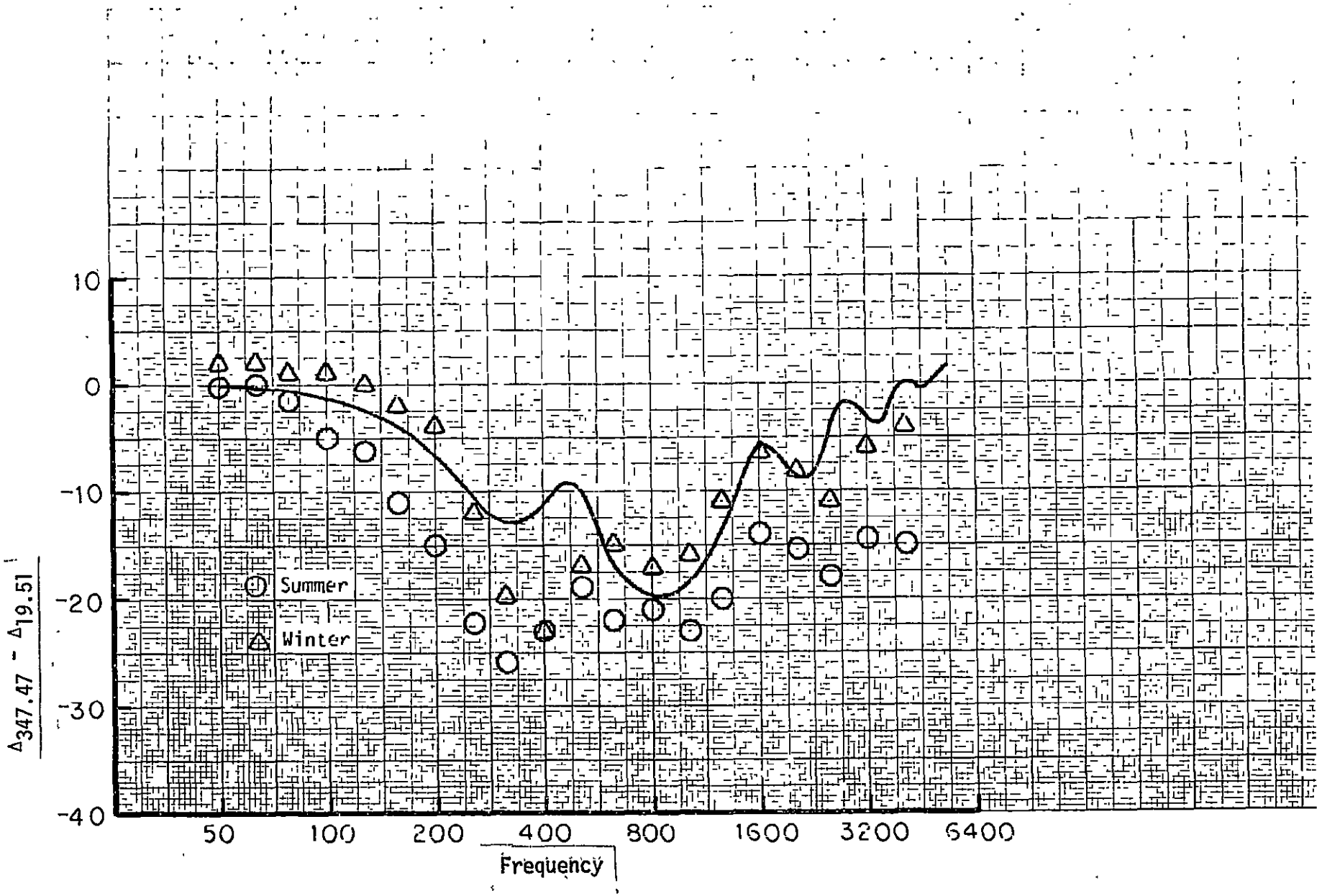

Figure 8. Comparison of Chien-Soroka theory to the Parkin and Scholes experimental data at Radlett. Ground admittance predicted by the Delaney and Bazley formula with assumed flow resistance of 2.5×10^5 N s/m^4.

e) 347.47 m microphone

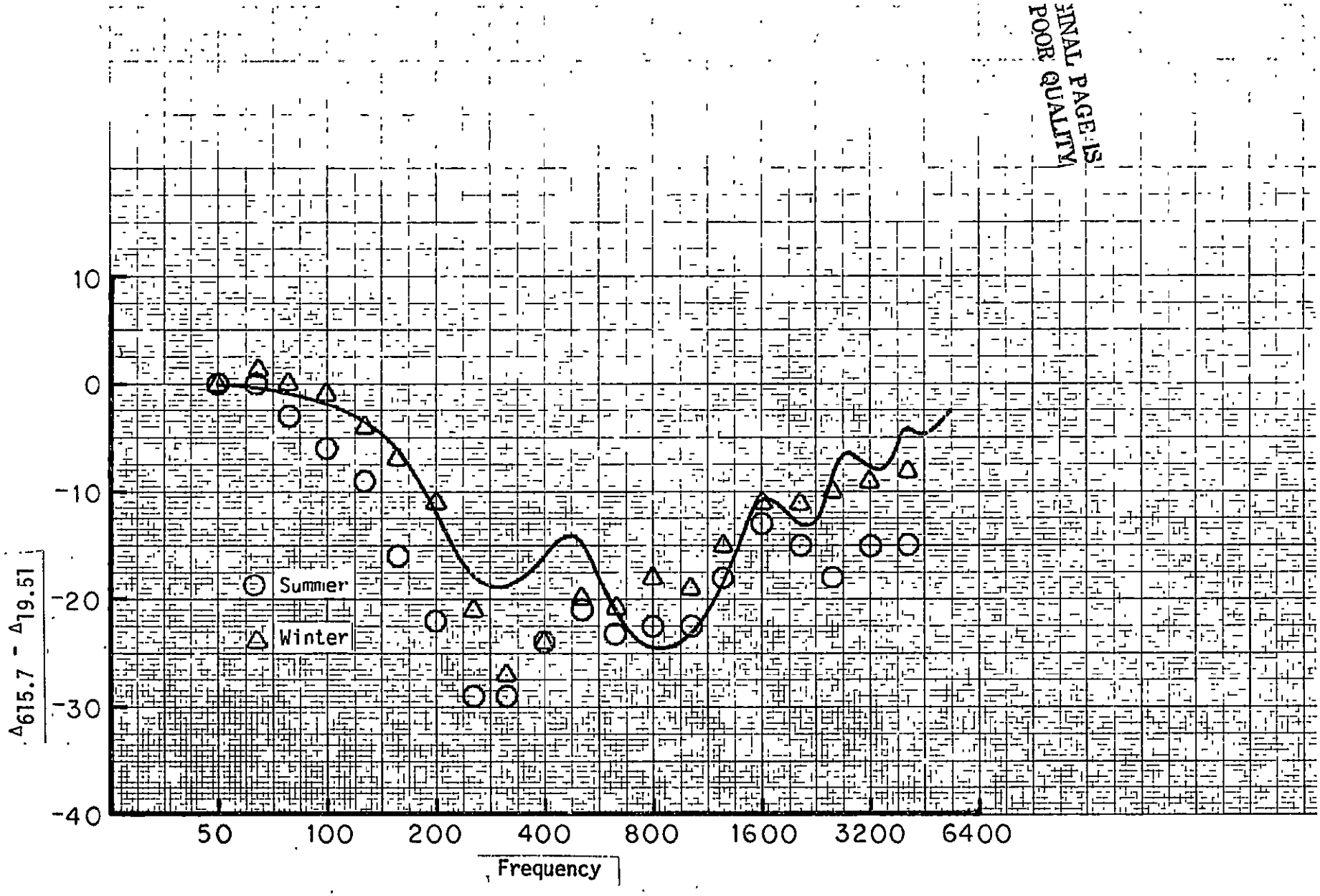

Figure 8. Comparison to Chien-Soroka theory to the Parkin and Scholes experimental data at Radlett. Ground admittance predicted by the Delaney and Bazley formula with assumed flow resistance of 2.5×10^5 N s/m^4.

f) 615.70 m microphone

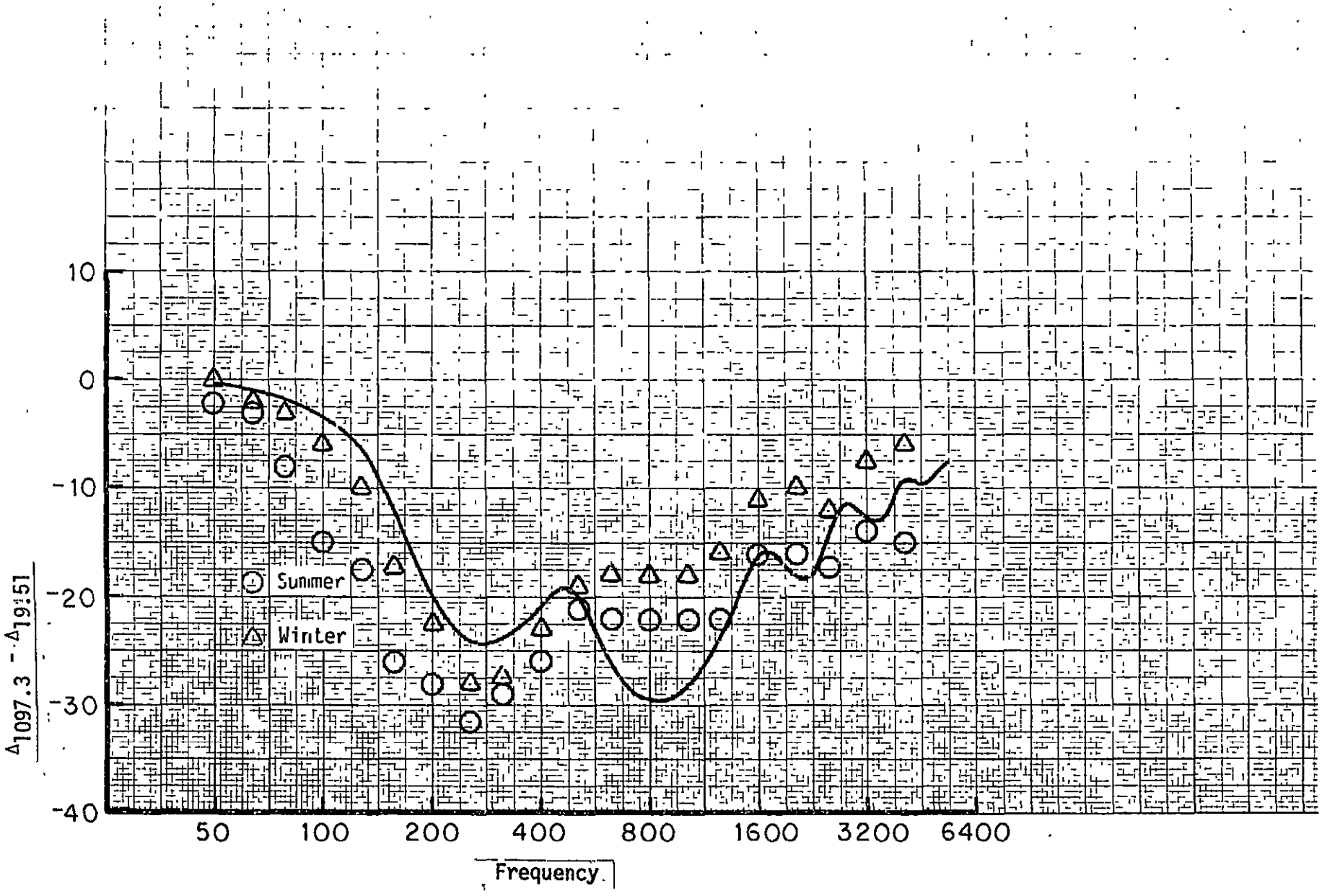

Figure 8. Comparison of Chien-Soroka theory to the Parkin and Scholes experimental data at Radlett. Ground admittance predicted by the Delaney and Bazley formula with assumed flow resistance of 2.5×10^5 N s/m^4.

g) 1097.3 m microphone

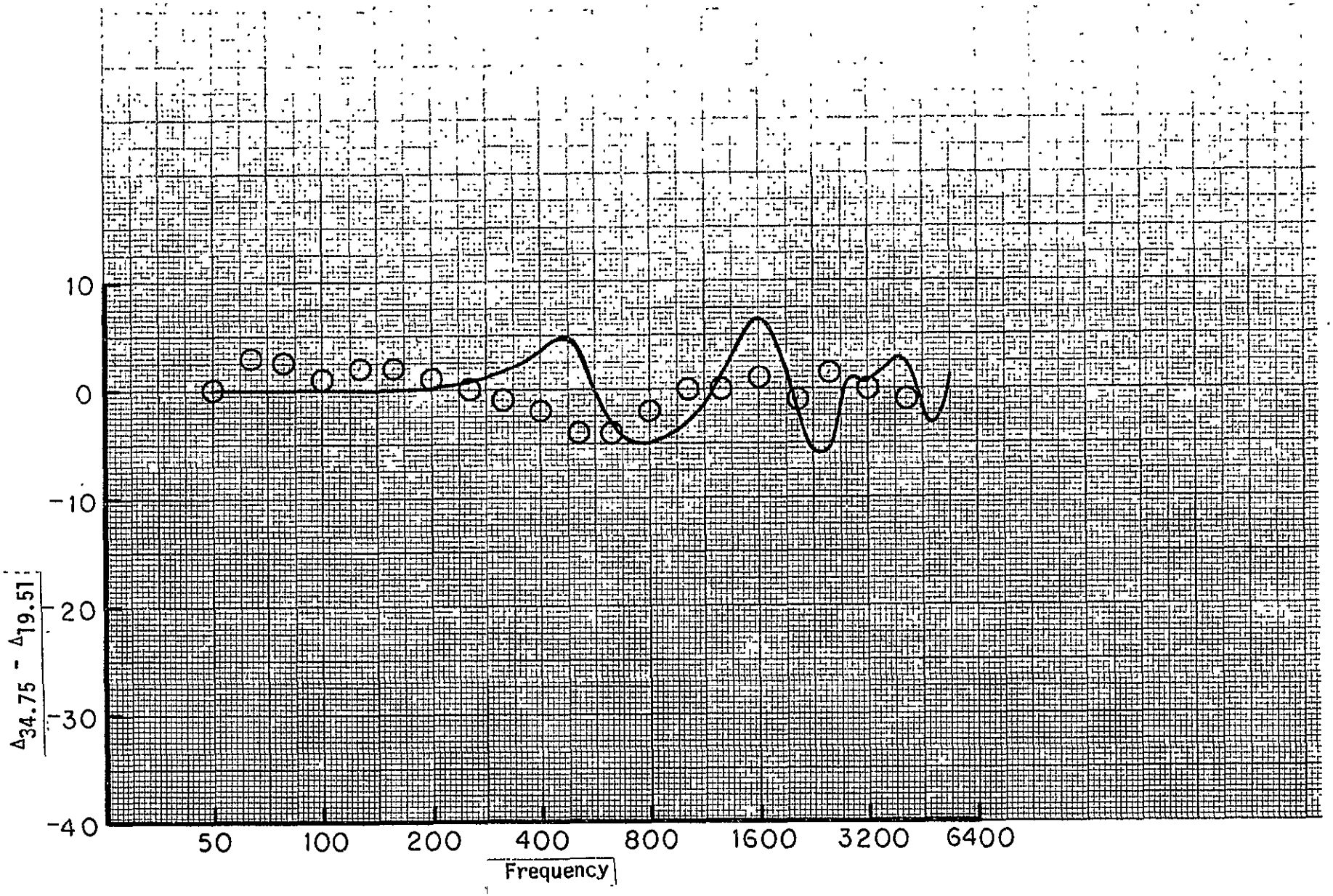

Figure 9. Comparison of Chien-Soroka theory to the Parkin and Scholes experimental data at Hatfield. Ground admittance predicted by the Delaney and Bazley formula with assumed flow resistance of 2.5×10^5 N s/m^4.

a) 34.75 m microphone

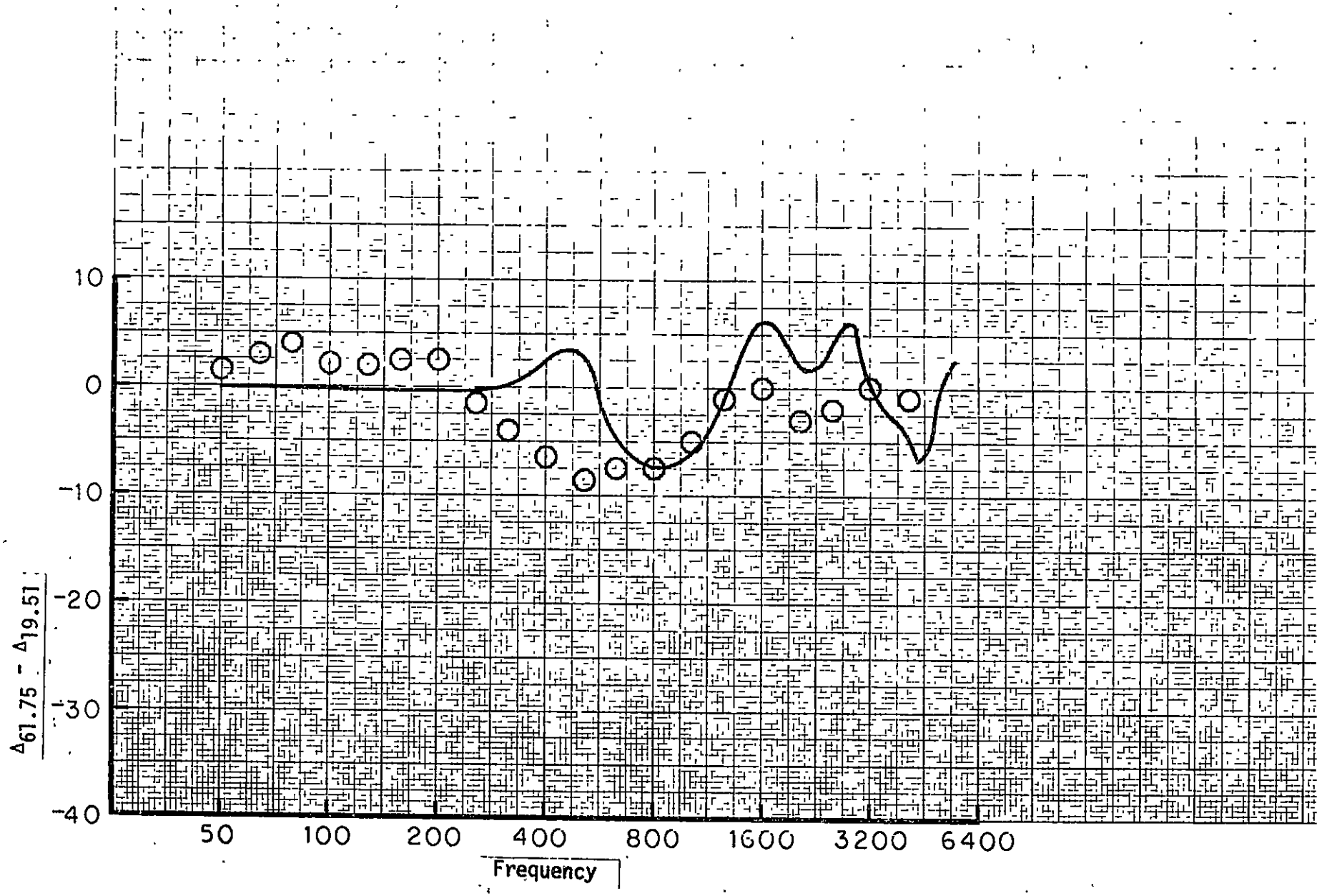

Figure 9. Comparison of Chien-Soroka theory to the Parkin and Scholes experimental data at Hatfield. Ground admittance predicted by the Delaney and Bazley formula with assumed flow resistance of 2.5×10^5 N s/m^4.

b) 61.75 m microphone

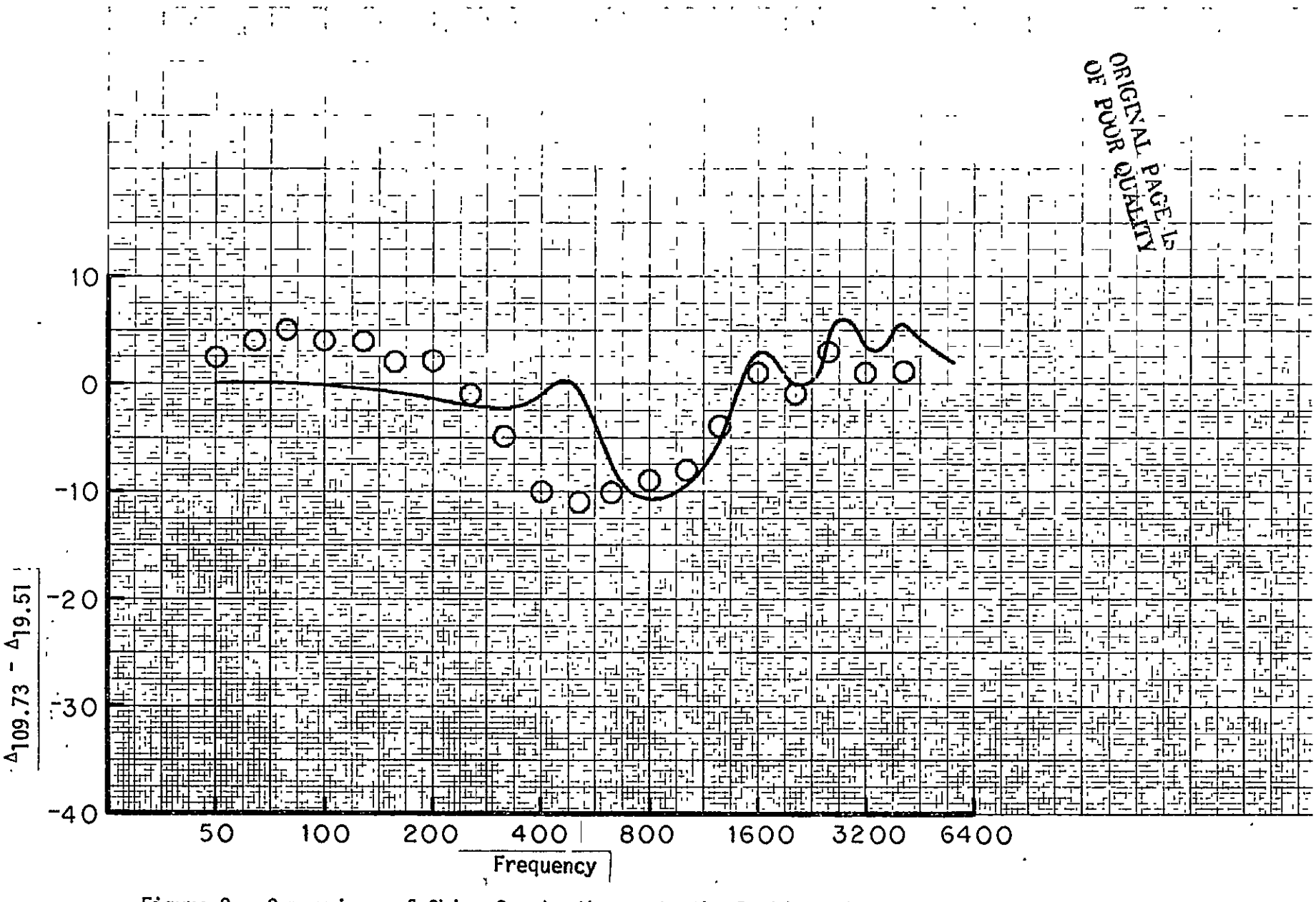

Figure 9. Comparison of Chien-Soroka theory to the Parkin and Scholes experimental data at Hatfield. Ground admittance predicted by the Delaney and Bazley formula with assumed flow resistance of 2.5×10^5 N s/m^4.

c) 109.73 m microphone

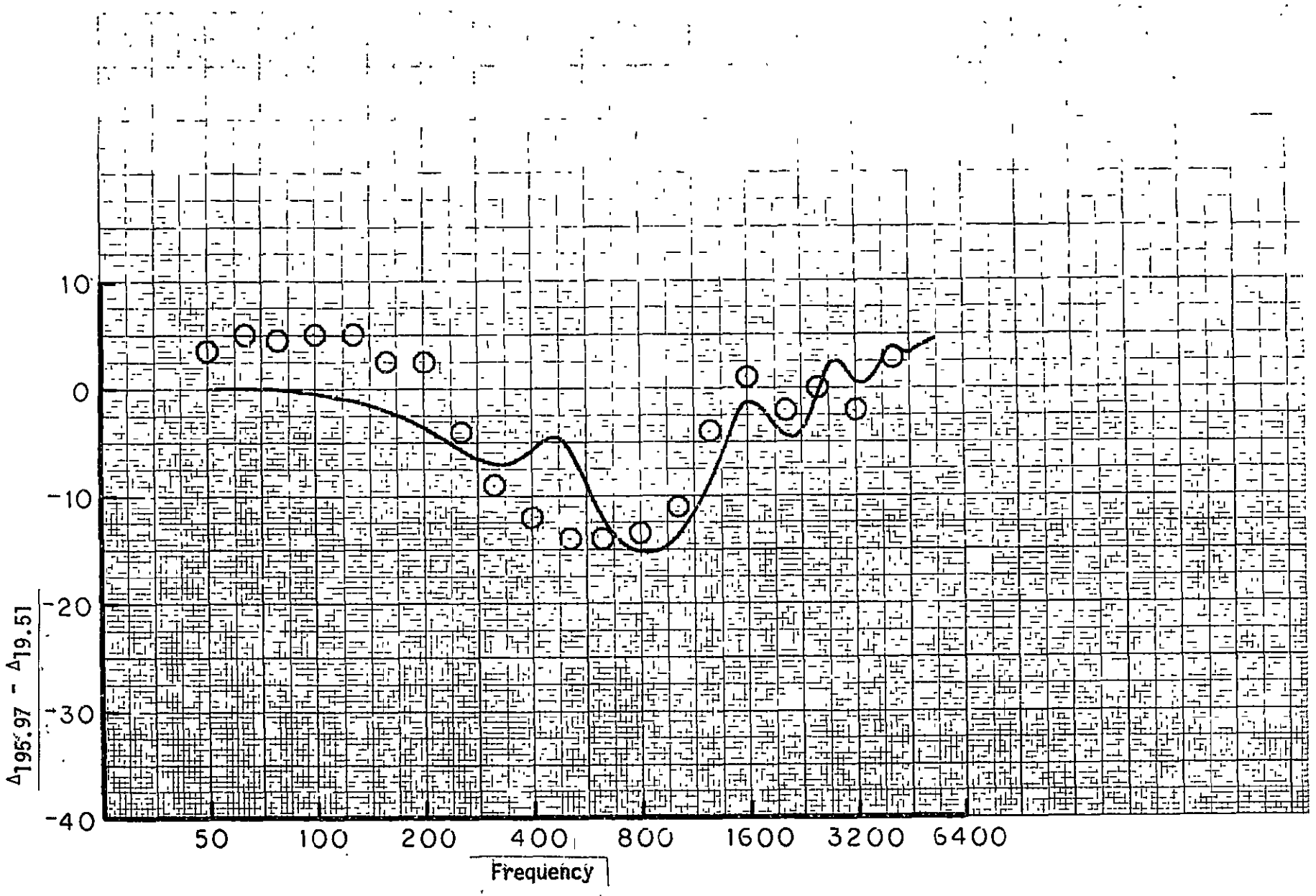

Figure 9. Comparison of Chien-Soroka theory to the Parkin and Scholes experimental data at Hatfield. Ground admittance predicted by the Delaney and Bazley formula with assumed flow resistance of 2.5×10^5 N s/m^4.

d) 195.97 m microphone

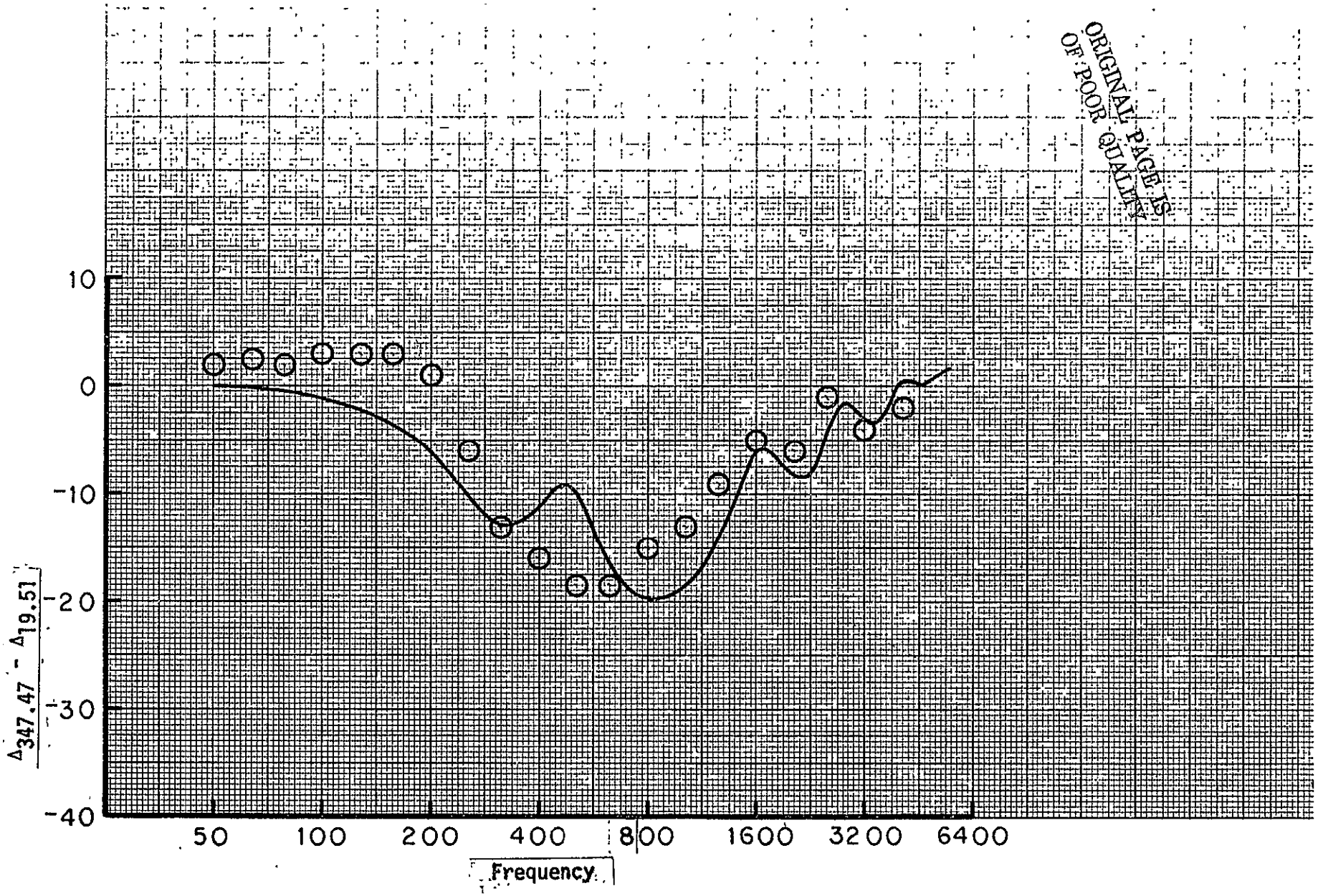

Figure 9. Comparison of Chien-Soroka theory to the Parkin and Scholes experimenatl data at Hatfield. Ground admittance predicted by the Delaney and Bazley formula with assumed flow resistance of 2.5×10^5 N s/m^4.

e) 347.47 m microphone

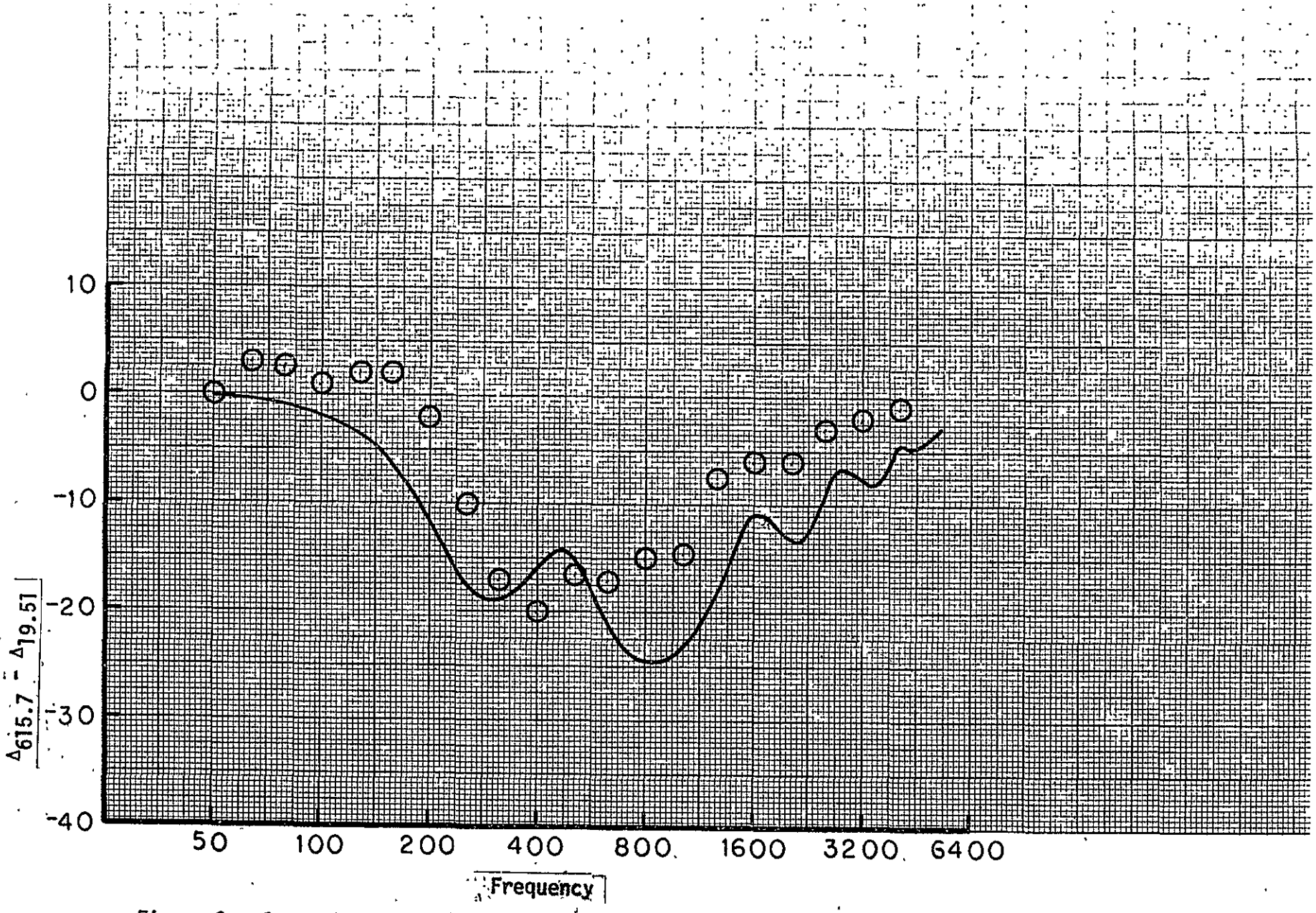

Figure 9. Comparison of Chien-Soroka theory to the Parking and Scholes experimental data at Hatfield. Ground admittance predicted by the Delaney and Bazley formula with assumed flow resistance of 2.5×10^5 N s/m^4.

f) 615.70 m microphone

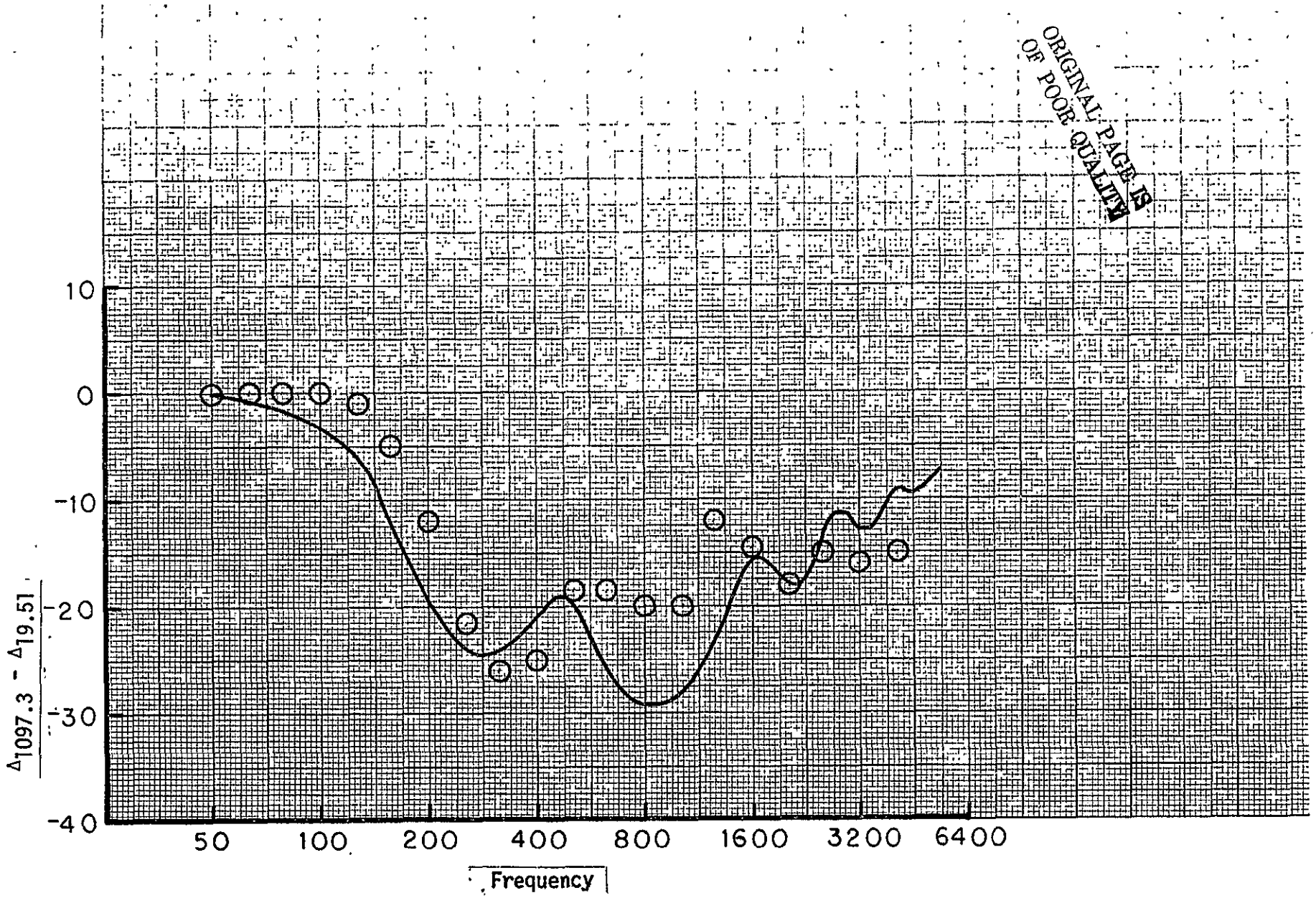

Figure 9. Comparison of Chien-Soroka theory to the Parkin and Scholes experimental data at Hatfield. Ground admittance predicted by the Delaney and Bazley formula with assumed flow resistance of 2.5×10^5 N s/m^4.

g) 1097.3 m microphone

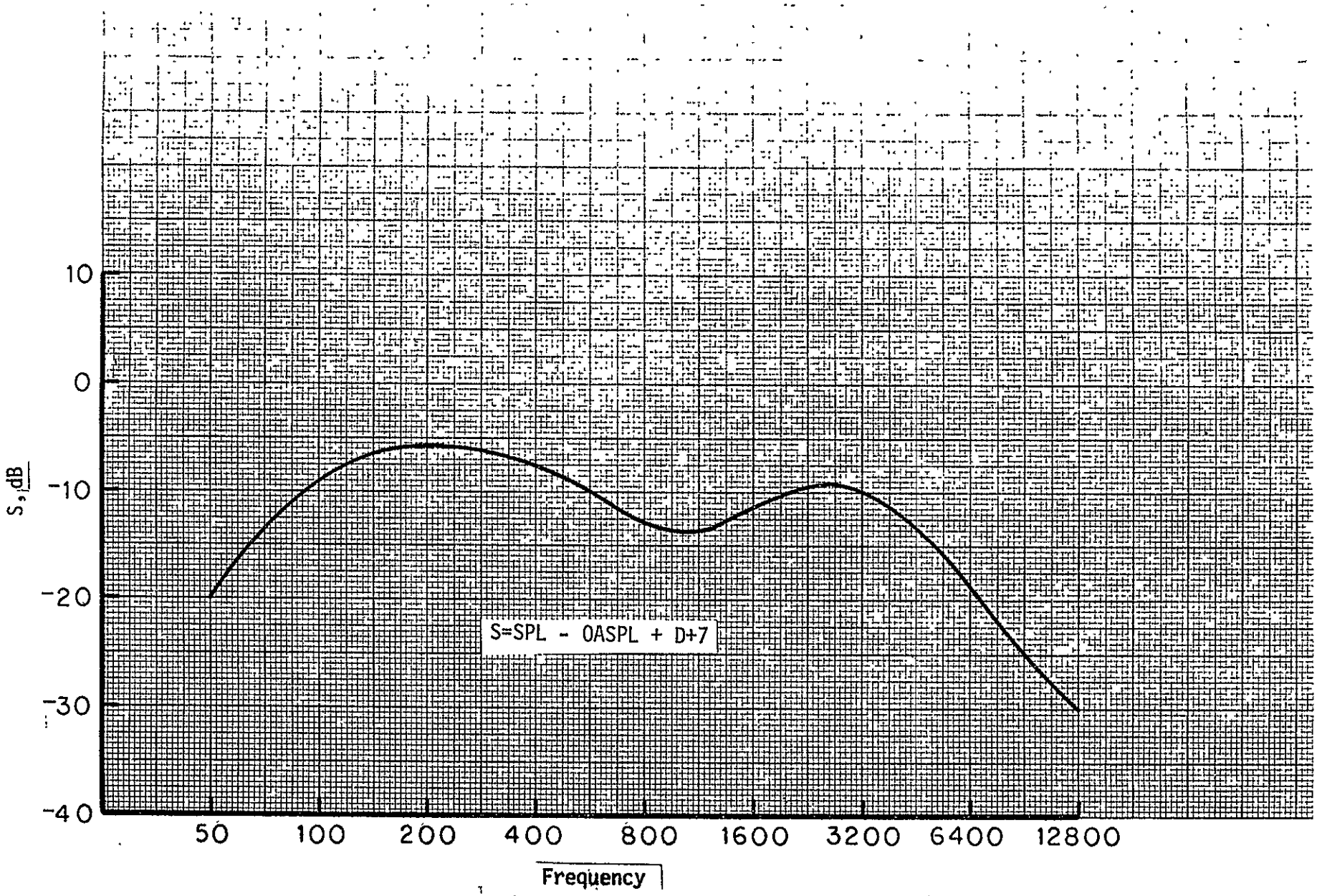

Figure 10. Estimated Concorde free-field jet mixing noise spectrum with D- weighting + 7 dB added for PNdB approximation.

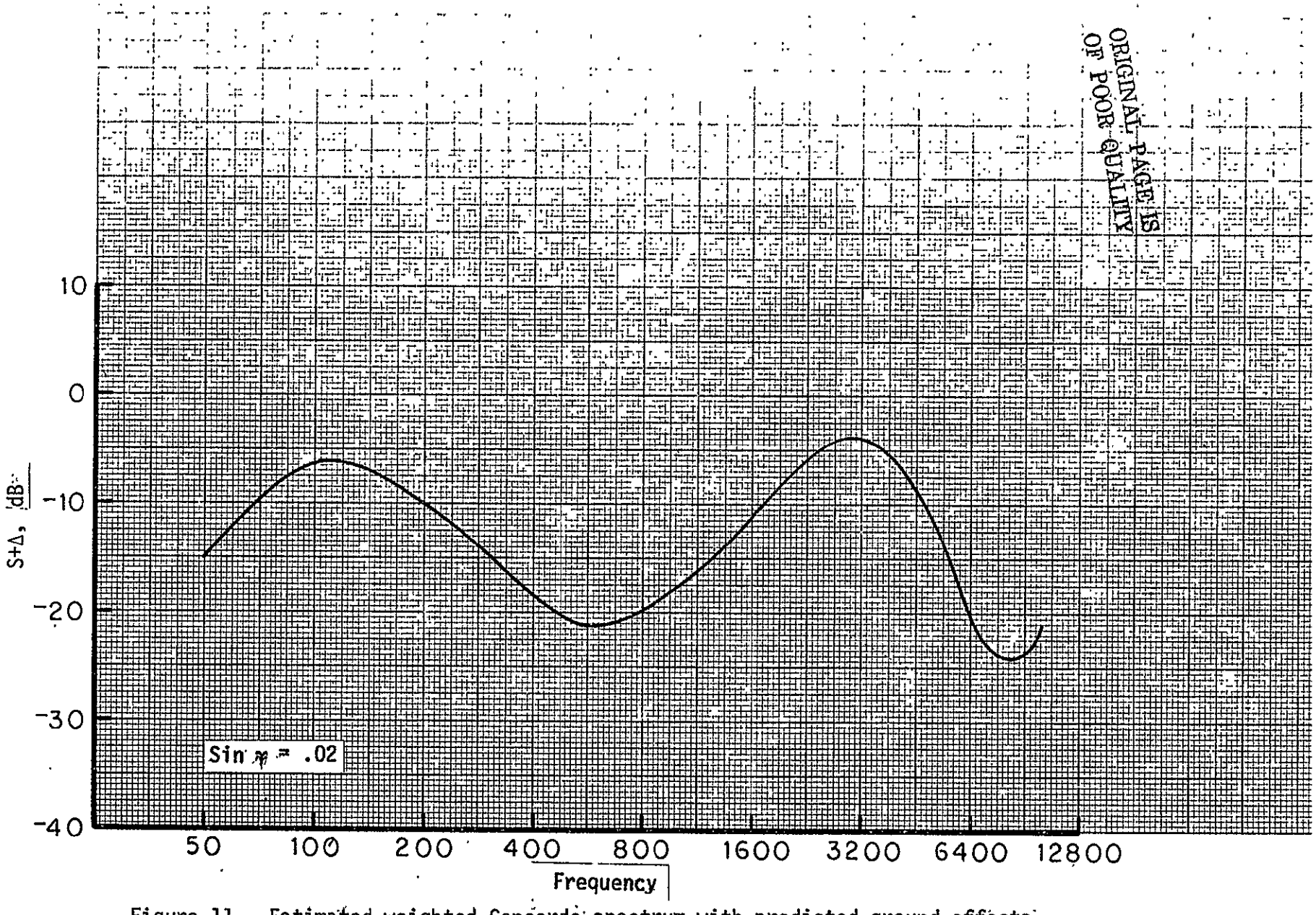

Figure 11. Estimated weighted Concorde spectrum with predicted ground effects at .35 n mi assuming flow resistance of 2.5×10^5 N s/m^4.

a) sin γ = .02

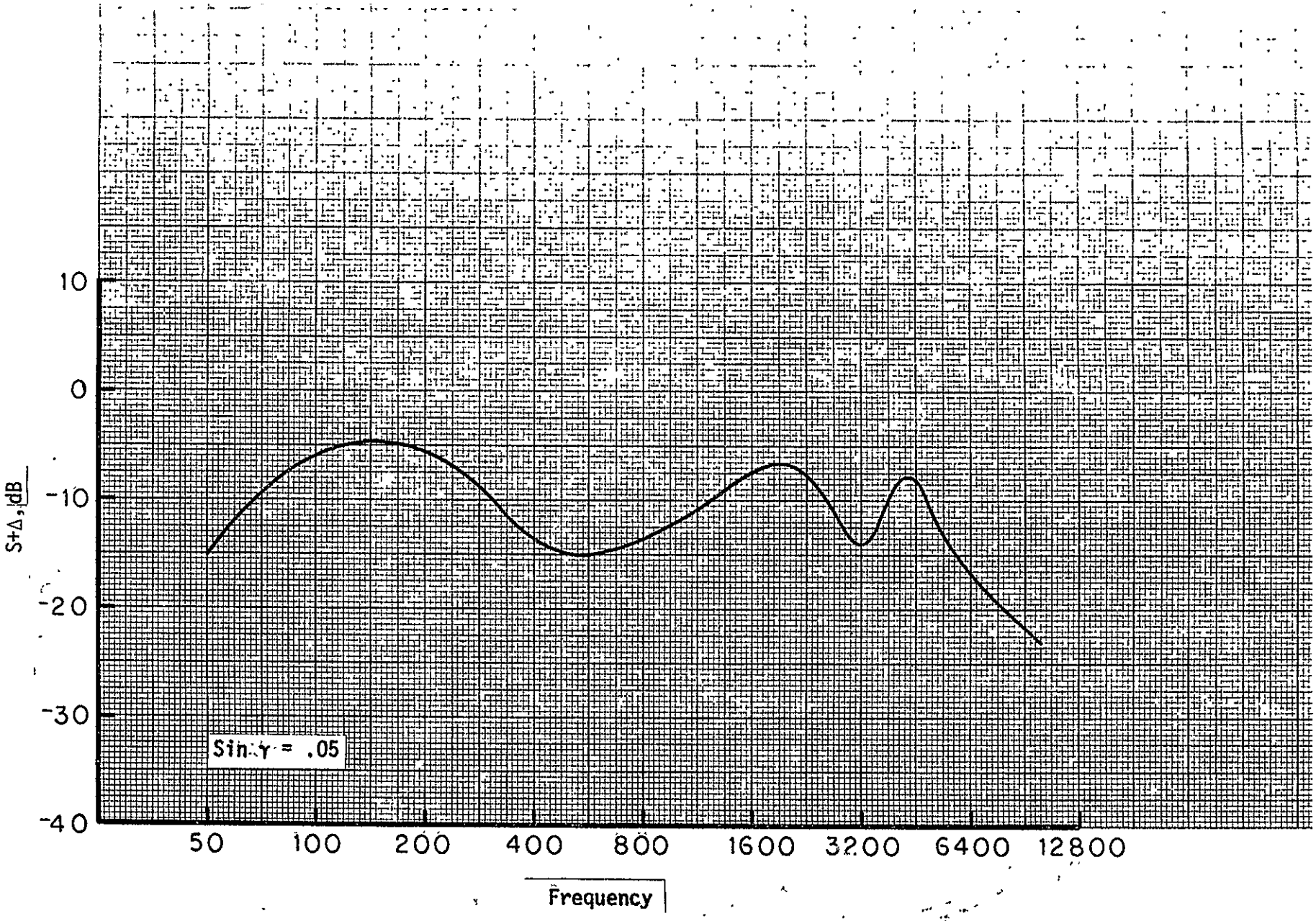

Figure 11. Estimated weighted Concorde spectrum with predicted ground effects at .35 n mi assuming flow resistance of 2.5×10^5 N s/m^4.

b) sin γ = .05

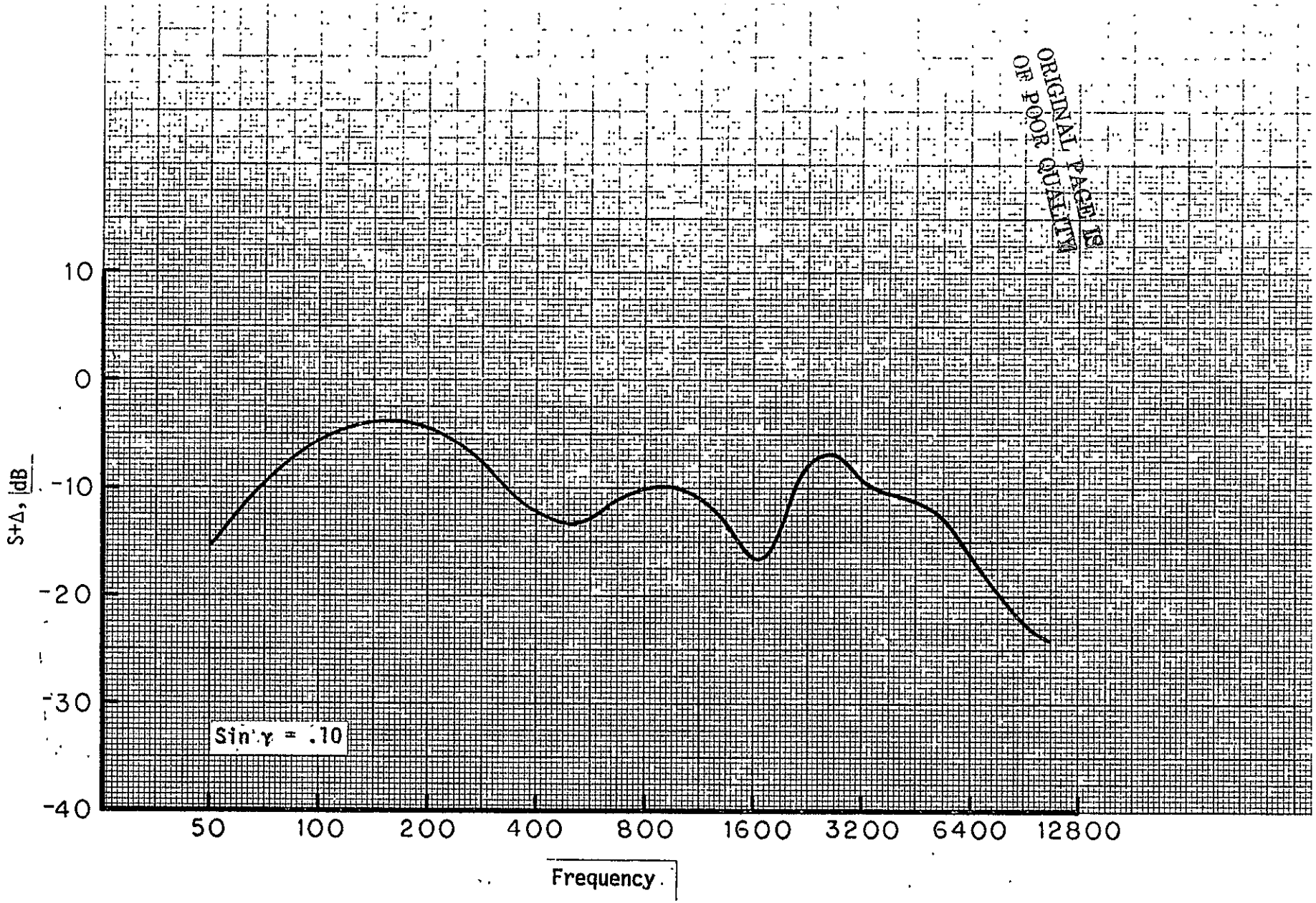

Figure 11. Estimated weighted Concorde spectrum with predicted ground effects at .35 n mi assuming flow resistance of 2.5×10^5 N s/m^4.

c) sin γ = .10

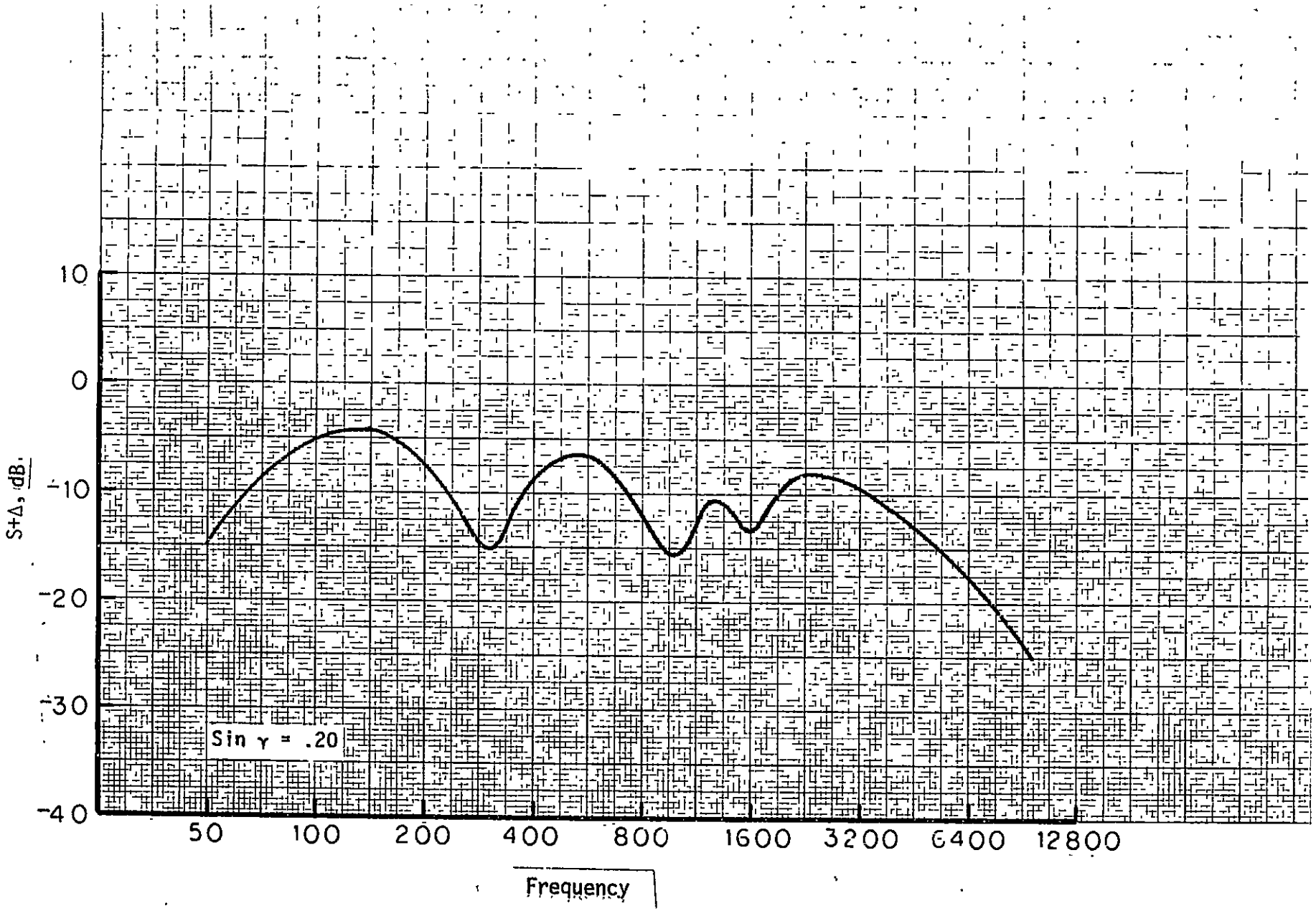

Figure 11. Estimated weighted Concorde spectrum with predicted ground effects at .35 n mi assuming flow resistance of 2.5×10^5 N s/m^4.

d) sin γ = .20

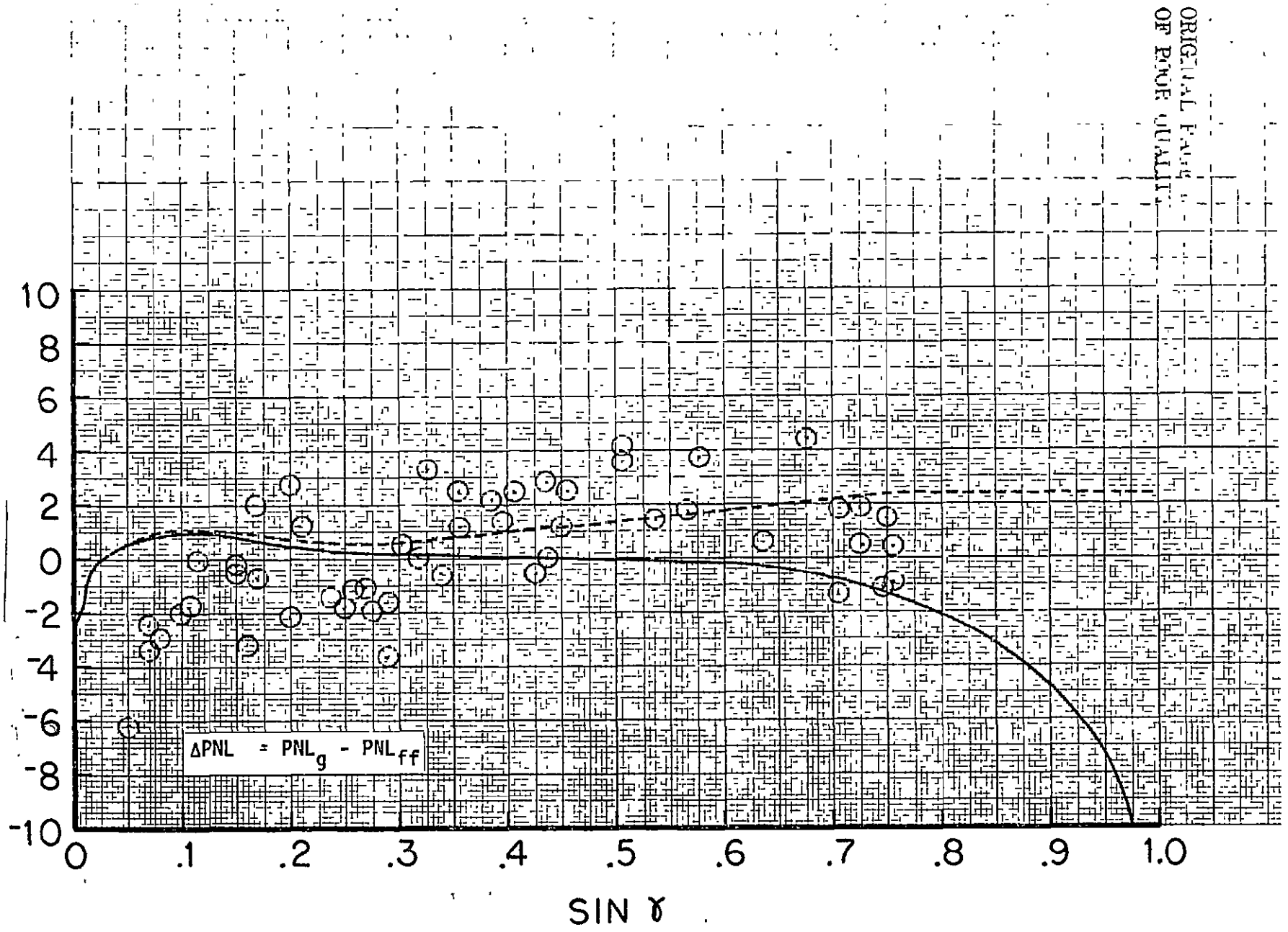

Figure 12. Comparison of predicted ground effect on estimated Concorde perceived noise to lateral attenuation data measured at .35 n mi sideline.

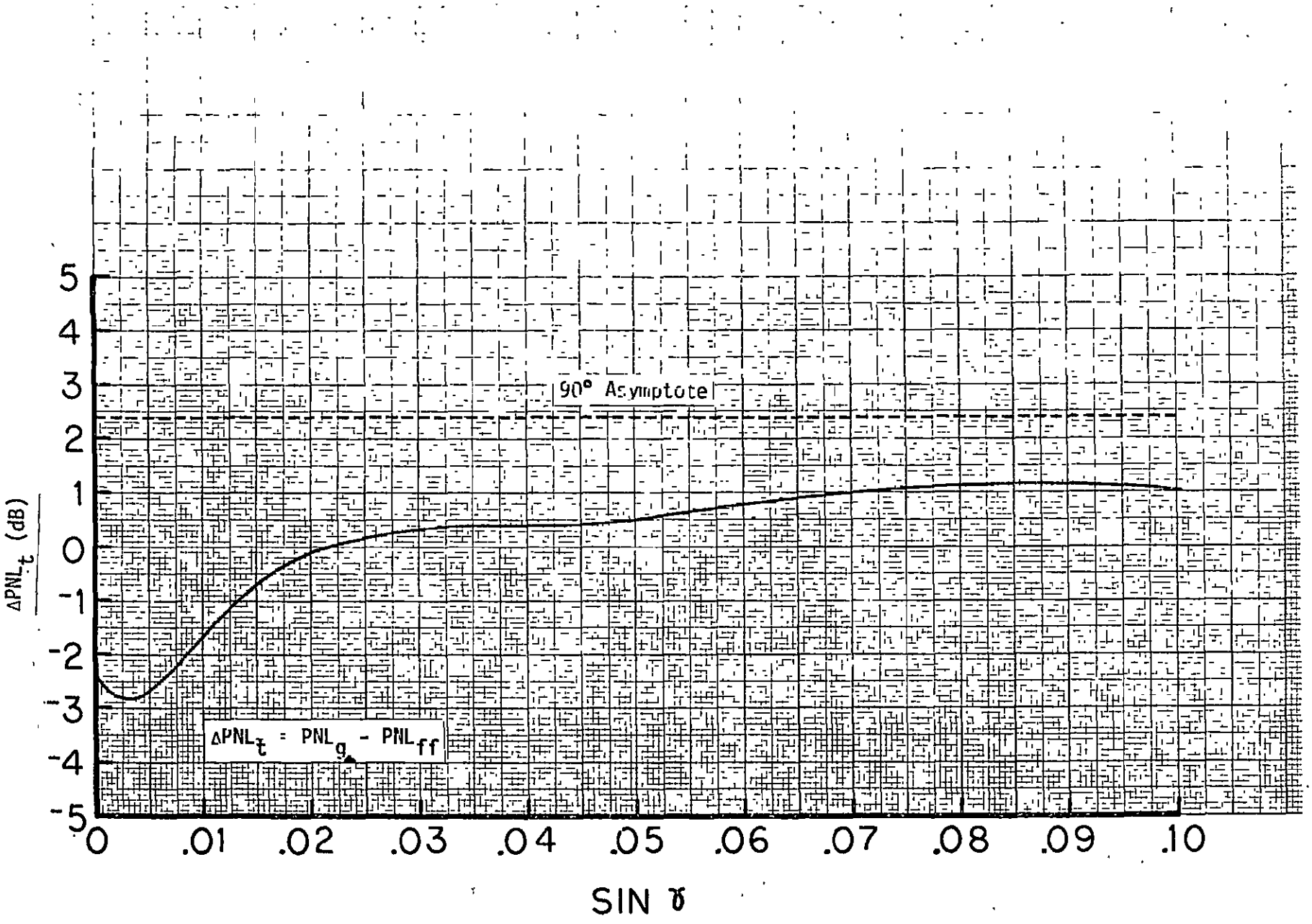

Figure 13. Ground attenuation of estimated Concorde perceived noise at low elevation angles. 1.2 m microphone at .35 n mi sideline with ground resistance of 2.5×10^5 N s/m^4.

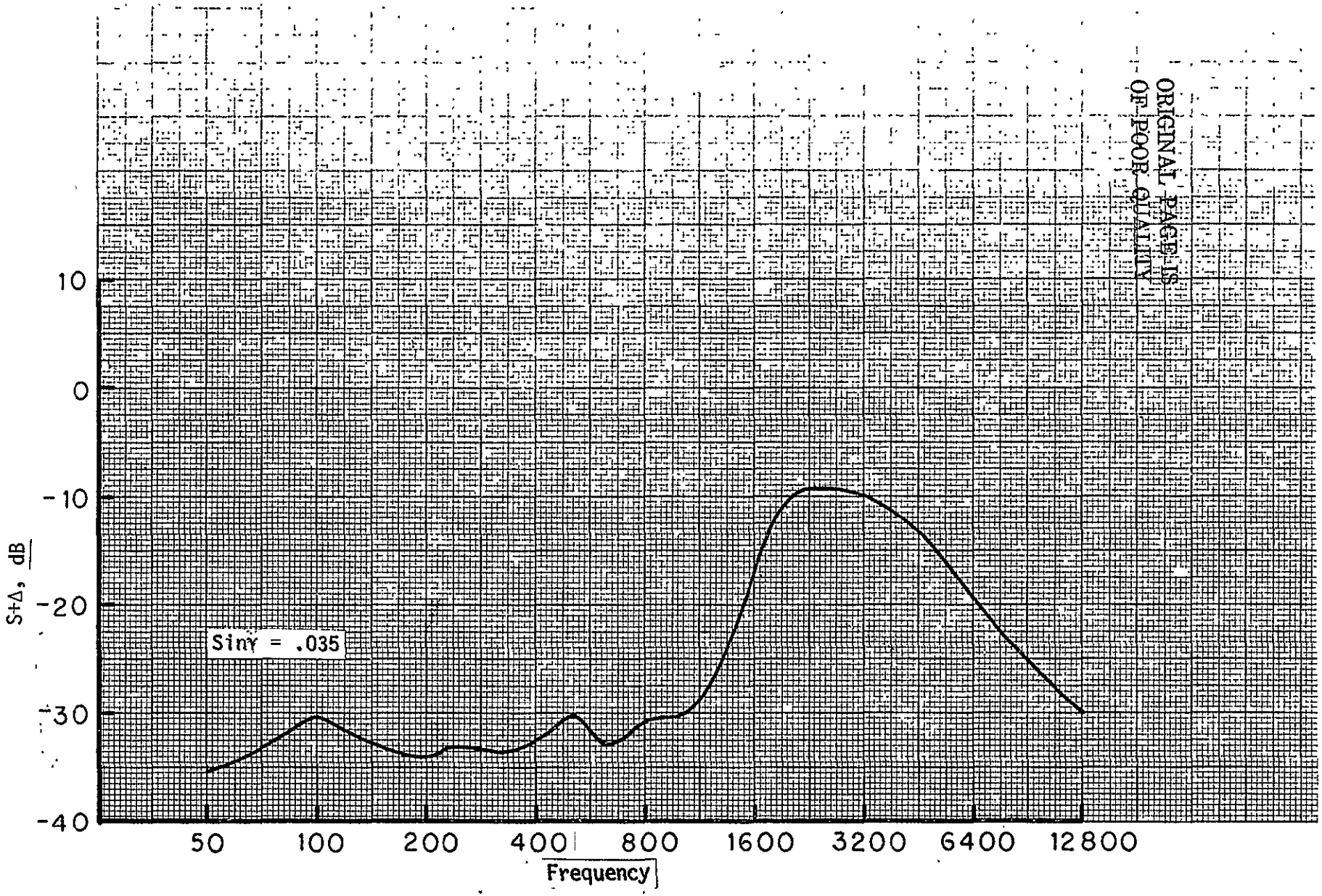

Figure 14. Estimated weighted Concorde spectrum with empirical ground attenuation effect (no reflection included) from reference 7.

a) $\sin \gamma = .035$

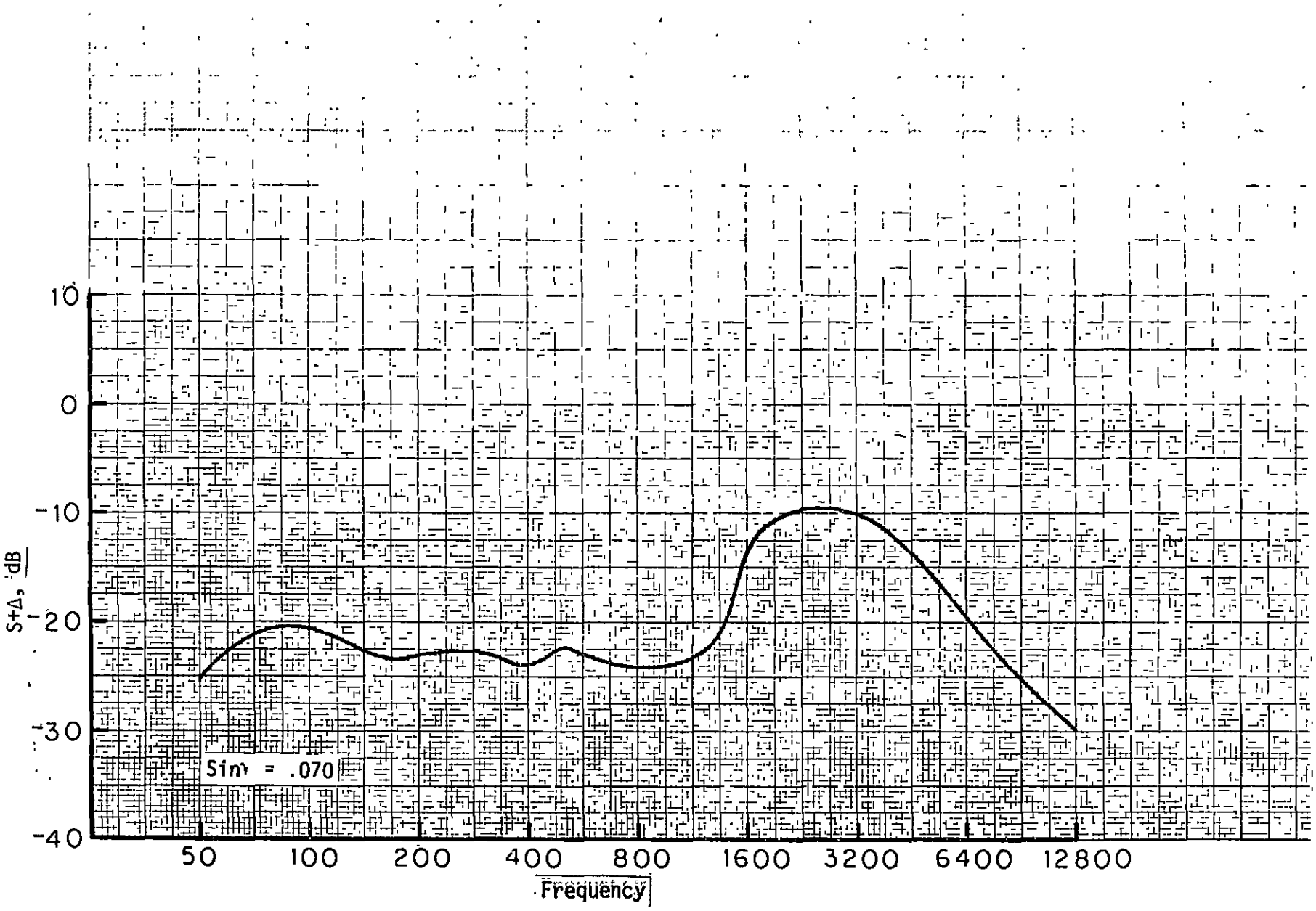

Figure 14. Estimated weighted Concorde spectrum with empirical ground attenuation effect (no reflection included) from reference 7.

b) sin γ= .070

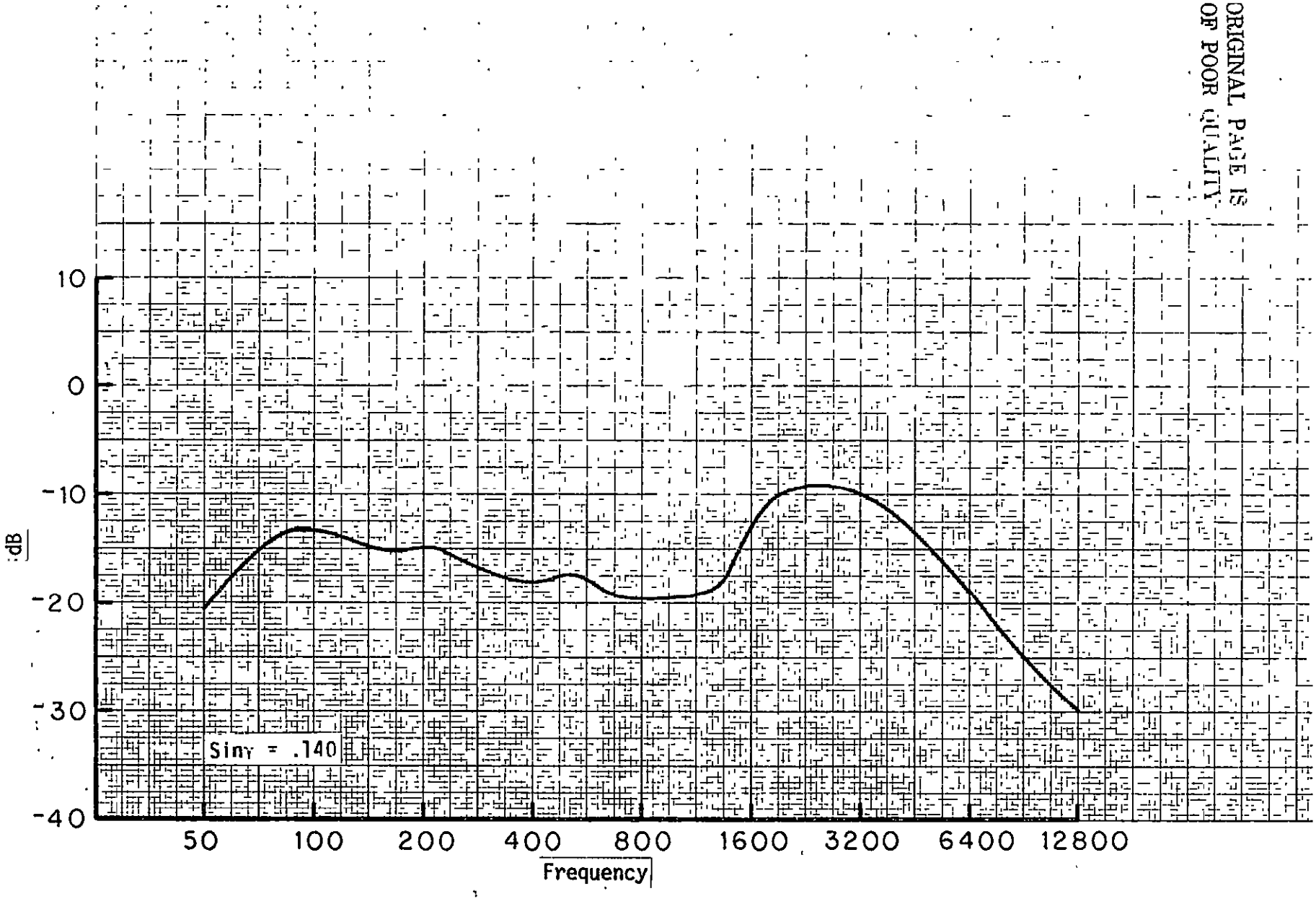

Figure 14. Estimated weighted Concorde spectrum with empirical ground attenuation effect (no reflection included) from reference 7.

c) sin γ= .140

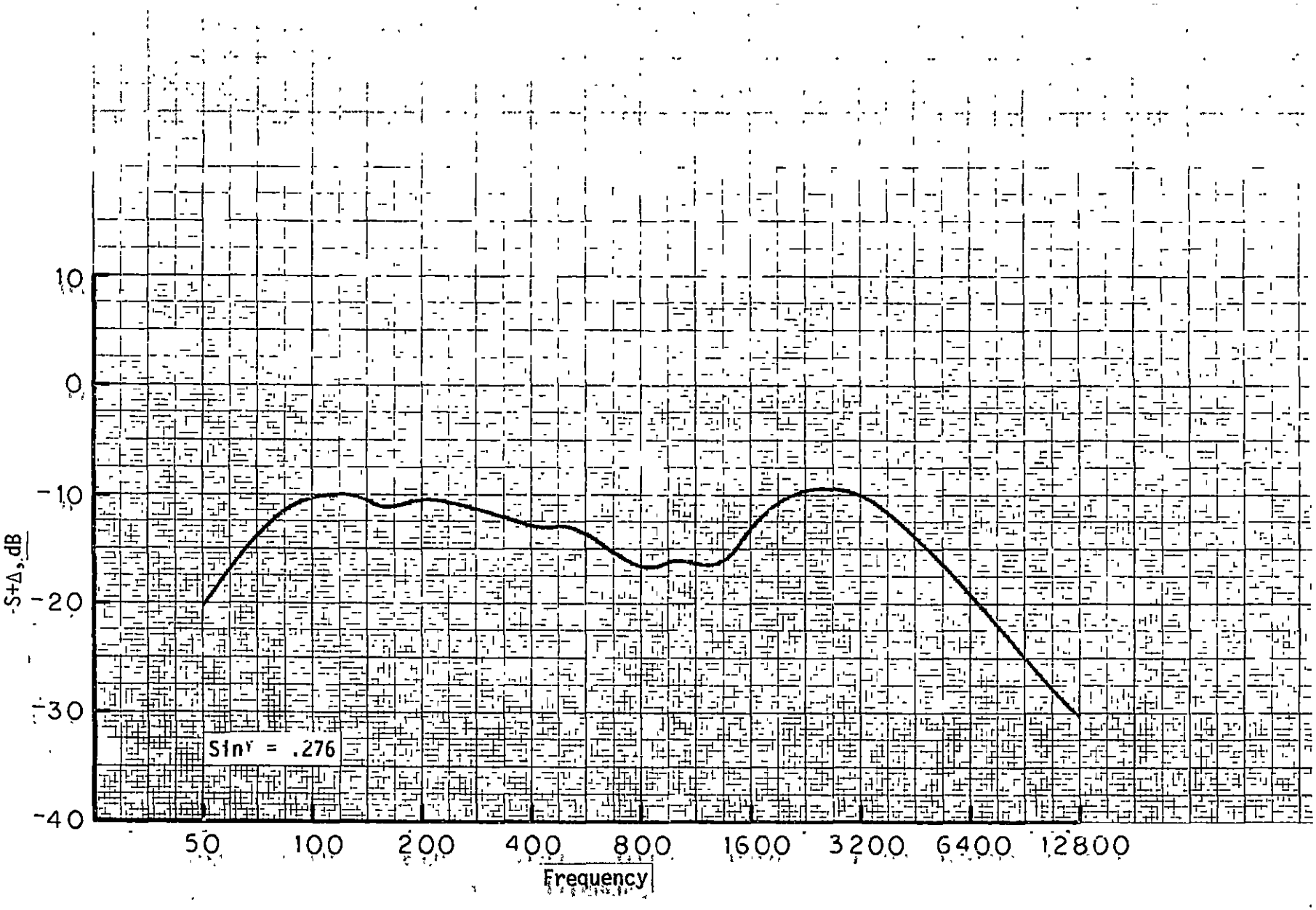

Figure 14. Estimated weighted Concorde spectrum with empirical ground attenuation effect (no reflection included) from reference 7.

d) sin γ = .276

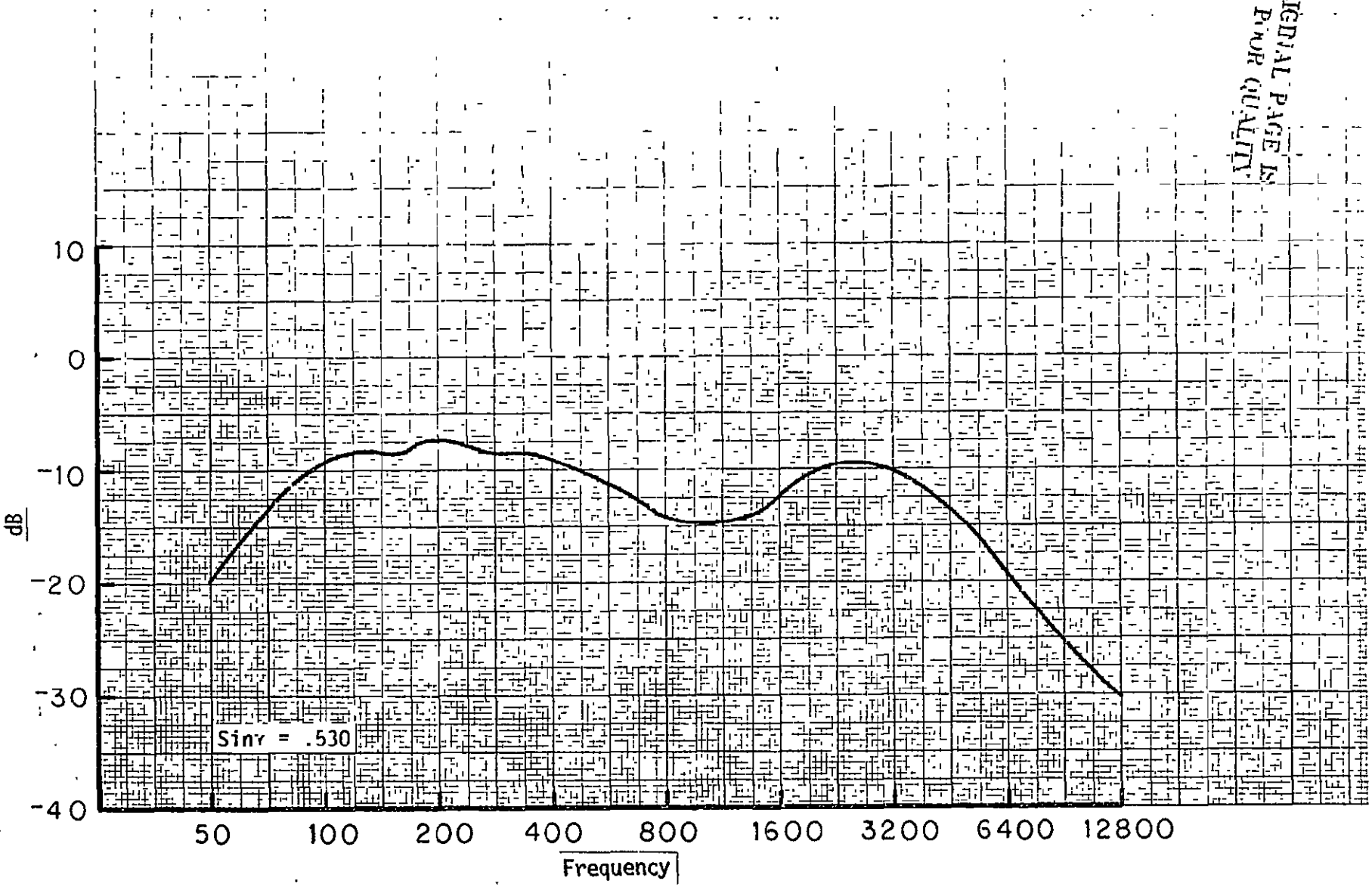

Figure 14. Estimated weighted Concorde spectrum with empirical ground attenuation effect (no reflection included) from reference 7.

e) $\sin \gamma = .530$

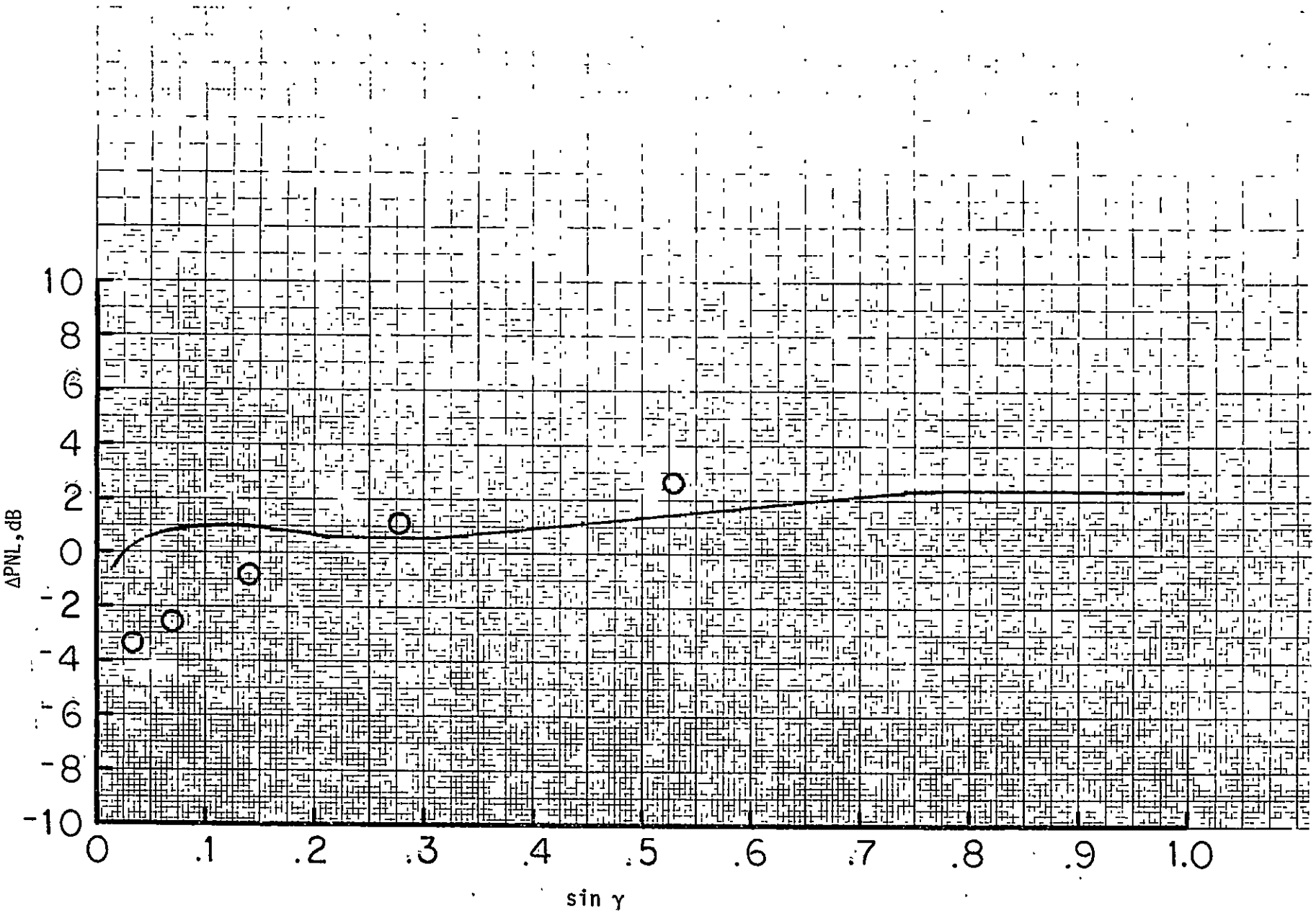

Figure 15. Comparison of empirical ground attenuation effect on Concorde perceived noise (no reflections included) to predicted effects.

1. Report No.	2. Government Accession No.	3. Recipient's Catalog No.
NASA TM-78717		

4. Title and Subtitle	5. Report Date
"Prediction of Aircraft Sideline Noise Attenuation"	June 28, 1978
	6. Performing Organization Code: 2650

7. Author(s)	8. Performing Organization Report No.
William E. Zorumski	
	10. Work Unit No.: 505-03-13-13
9. Performing Organization Name and Address: NASA Langley Research Center, Hampton, Virginia 23665	11. Contract or Grant No.
	13. Type of Report and Period Covered: Technical Memorandum
12. Sponsoring Agency Name and Address: National Aeronautics and Space Administration, Washington, D. C. 20546	14. Sponsoring Agency Code

15. Supplementary Notes

16. Abstract

A computational study is made using the recommended ground effect theory by Pao, Wenzel, and Oncley. It is shown that this theory adequately predicts the measured ground attenuation data by Parkin and Scholes, which is the only available large data set. It is also shown, however, that the ground effect theory does not predict the measured lateral attenuations from actual aircraft flyovers. There remain one or more important lateral effects on aircraft noise, such as sideline shielding of sources, which must be incorporated in the prediction methods. Experiments at low elevation angles (0^{o} to 10^{o}) and low-to-intermediate frequencies are recommended to further validate the ground effect theory.

17. Key Words (Suggested by Author(s))	18. Distribution Statement
Noise prediction	Unclassified Unlimited

19. Security Classif. (of this report)	20. Security Classif. (of this page)	21. No. of Pages	22. Price*
Unclassified	Unclassified	50	$4.50

* For sale by the National Technical Information Service, Springfield, Virginia 22161